Exploring the anti-leukemic effect of the combination treatment with Valproic acid, Lonidamine and Mycophenolate mofetil in acute myeloid leukemia

Carina Hinrichs

Master`s Degree

This thesis is submitted in partial fulfilment of the requirements for the degree of Master of Science in Medical Biology – Medical Cell Biology. The work was conducted at Section for Hematology, Clinical Institute II, University of Bergen.

Department of Biomedicine and Department of Clinical Science
University of Bergen, Norway

June 2015

Acknowledgement

I would like to first and foremost sincerely acknowledge my head supervisor Dr. Rakel Brendsdal Forthun for inviting me to the Translational Hematology and Oncology Group at the Department of Clinical Science and University of Bergen. Not only has her continued support and encouragement kept me motivated and saved a lot of sleepless nights, but her scientific knowledge and thoroughly proofreading also inspired me to strive for a better understanding of my thesis and cancer research. I would also like to thank my co-supervisor Professor Bjørn Tore Gjertsen for including me into his research group and into the scientific environment. I truly appreciate the way Bjørn Tore Gjertsen has guided me through my studies and the attention he has given me and my work.

I am most thankful to all of the colleagues of the Gjertsen laboratory for their good advises, technical help and especially for lighten up the scientific workplace. Wenche Eilifsen and Siv Lise Bedringaas are appreciated for their helping hand they have given me when I was “lost” in the laboratory. Andrè Sulen is thanked for his patience on introducing and training me for flow cytometry. In addition I would like to thank Maria Omsland for showing me how to use the microscope and Calum Leitch for being so kind proof-reading parts of my thesis.

I am truly thankful to all my friends who have supported me and even cooked for me during this thesis. I also wish to point out and acknowledge Tara Helen Dowling for her continued friendship throughout the thesis and of that which is going to be continued.

And at last but not least, my truly and specially thanks goes to my family who helped me stay sane through this project and never hung up on a phone call.

Bergen, June 2015

Carina Hinrichs

Contents

Acronyms and abbreviations

6-MP	6-mercaptopurine
Allo-SCT	Allogeneic-stem cell transplantation
APL	Acute promyeloid leukemia
APS	Ammonium persulfate
ATRA	all-trans-retinoic acid
Auto-SCT	Autologous-stem cell transplantation
BNML	Brown Norwegian Myeloid leukemia
BSA	Bovine serum albumin
CR	Complete remission
DAPI	4', 6-diamidino-2-phenylindole
GMP	Guanosine monophosphate
Flt3	Fms-like tyrosine kinase 3
HDAC	Histone deacetylase
HK	Hexokinase
HPRT1	Hypoxanthine phosphoribosyltransferase
HSC	Hematopoietic stem cell
HU	Hydroxyurea
IgG	Immunoglobulin G
IMAC	Immobilized med affinity chromatography
IMP	Inosine 5`- monophosphate
IMPDH	Inosine monophosphate dehydrogenase
i.p.	Intraperitoneal
LND	Lonidamine
MTD	Maximum tolerated dose
NSG	NOD/scid/gamma
PBMC	Peripheral blood mononuclear cell
PBS	Phosphate buffered saline
Poly (ethylene glycol)	PEG
SDS	Sodium dodecyl sulfate
TEMED	N, N, N', N'-Tetramethylethylenediamine
TBS-T	Tris-Buffered Saline with Tween-20
VDAC	Voltage dependent anion channel

(v/v)	volume by volume
XMP	xanthosine monophosphate

Summary

An accumulation of immature myeloid progenitor cells at the expense of normal hematopoietic precursors characterizes the aggressive heterogeneous cancer acute myeloid leukemia (AML). It affects the bone marrow and peripheral blood leading to defects in myeloid cell function. (1) The median age of patients with AML is 67 years and the side effects associated with chemotherapy available today can often not be tolerated by this subgroup of patients. (2) Thus, new alternative therapeutic strategies are needed. Valproic acid (VPA) has shown an anti-leukemic effect in 20% of AML patients. The beneficial effect on survival in the Brown Norwegian Myeloid Leukemia (BNML) syngeneic rat leukemia model when treated with the compound was previously investigated and the phosphoproteomic study revealed differentially expressed proteins following VPA treatment. (3) The expression of hexokinase 1 (HK1) and hypoxanthine phosphoribosyltransferin 1 (HPRT1) was reduced by VPA. These proteins are inhibited by the drugs Lonidamine (LND) and Mycophenolate mofetil (MMF), respectively, (4, 5) and were for that reason explored for their anti-leukemic effect and in combination with VPA to enhance AML patients' responsiveness. The ability of MMF to induce cell growth inhibition in three human AML cell lines was assessed and the cooperation of VPA and LND to reduce cell proliferation by synergism was revealed by WST-1 proliferation based assay, Hoechst 33342 dsDNA staining and Annexin-V/PI flow cytometric analysis. Signaling pathways were investigated by Western blot, and a pilot study in NOD/scid/gamma (NSG) mice was performed for estimating the maximum tolerated dose (MTD) of LND.

The combination studies of VPA with LND or MMF are novel in AML. Novel agents are hoped for that they will augment the current chemotherapy available for AML patients to overcome drug resistance pathways, and to eventually improve the outcomes for those patients. The observations made may aid in the identification of targeted treatment with combination therapy for individual AML patients. This thesis demonstrates the use of metabolically interfering drugs for a dose-dependent suppression of human AML cell lines and the subsequent viability assays.

1. Introduction

Acute myeloid leukemia (AML) is an aggressive heterogeneous cancer of the peripheral blood and the bone marrow, represented by a clonal expansion and accumulation of immature myeloid progenitor cells (blasts). (1) This loss of normal hematopoietic proliferation and differentiation leads to defects in myeloid cell function resulting in anemia, increased bleeding, higher infection risk, as well as organ infiltration of leukemic blasts. (1) Intensive chemotherapy consists most often of 7 days standard doses cytarabine, and 3 following days of anthracycline, also known as the 7 + 3 day regimen. The triphosphate derivative of the antimetabolite cytarabine inhibits DNA polymerase, whereas anthracyclines are cytotoxic antibiotic compounds by direct action on DNA. (6) Other chemotherapeutic agents are usually incorporated to the 7+3 regimen and followed by courses of consolidation chemotherapy or allogeneic stem cell transplantation (SCT). (7) The 7+3 regimen of cytarabine and the anthracycline daunorubicin has since 1973 been standard therapy of AML. (8)Age is a major determinant of outcome in AML patients following treatment. The median age of patients with AML at diagnosis is 67 years, presenting the most common leukemia in adults. The age-adjusted population incidence is 17.5 per 100 000 for people 65 or older, compared to 1.8 people in 100 000 for those younger than 65 years. (2, 9) Increasing age is associated with decreased immune-responsiveness that makes older patients tolerate infections to lesser extent. Slower drug clearance observed in older AML patients may contribute to increased chemotherapy toxicity. (10) And other factors influencing the aging population can be that they are more likely to have comorbidities and more adverse cytogenetics is also observed with increased age. (11)

In the late 1970 when the development of new drugs for treating leukemia took place, the 5-year overall survival was as low as 6.2% for patients in all races, sexes and all ages. This percentage increased to 25.8% in the year of 2010 according to The National Institute of Health: SEER Cancer Statistics. (2) However, when considering the age at diagnosis, the statistics changes considerably. From the year of 2004 to 2010, patients younger than 45 years of age had a 5-year relative survival of 55.6%, whereas the numbers are only 5.6% for patients aged 65 years and above. (2) It is therefore evident for the need of new therapy aiming this group of patients.

1.1 Diagnosis and Classification

Acute myeloid leukemia needs to be diagnosed accurately to distinguish it from myelodysplastic syndromes (MDS) and lymphatic leukemia, as these diseases have great differences in prognosis as well as therapeutic strategies and effectiveness of therapy. (12) Procedures in the initial diagnosis include complete blood count (CBC) and peripheral blood smear, bone marrow aspiration (marrow) and biopsy (bone and marrow), immunophenotyping and cytogenetic analysis or reverse transcription polymerase chain reaction (RT-PCR) analysis to investigate gene fusions and somatically acquired mutations. (13) The diagnostic tests provide information allowing classification if the malignancies into subgroups relevant for treatment option or prognosis. Two classification systems of AML exist; the first developed by the French-American-British (FAB) Cooperative group and the more recent and generally accepted World Health Organization (WHO) classification system. (13) The FAB classification accounts mainly for morphological characteristics analyzed by cytochemistry and immunophenotyping. These are still important in the WHO classification, which in addition is based on genetic abnormalities and clinical characteristics (**Table 1**). According to WHO a percentage of 20 or more of leukemic blasts in the peripheral blood or bone marrow is required for the diagnosis of AML. However, patients with the cytogenetic abnormalities; RUNX1-RUNX1T1 (t(8;21)(q22;q22)), CBFB-MYH11 (inv(16)(p13.1q22) or t(16;16)(p13.1;q22)), PML-RARA (t(15;17)(q22;q12) are always considered to have AML, disregarding the percentage of blasts. (13, 14)

Tabel 1. The 4th edition WHO classification of Acute Myeloid Leukemia, updated in 2008

AML with recurrent genetic abnormalities
AML with t(8;21)(q22;q22), RUNX1-RUNX1T1
AML with inv(16)(p13.1q22) or t(16;16)(p13.1;p22); CBFB-MYH11
Acute promyelocytic leukemia with t(15;17)(q22;q12);PML-RARA
AML with t(9;11)(p22;q23)MLLT3-MLL
AML with t(6:9)(p23;q34); DEK-NUP214
AML with inv(3)(q21q26.2) or t(3.3)(q21;26.2); RPN1-EVl1
AML (megakaryoblastic) with t(1:22)(p13;q13); RBM15-MKL1
AML with mutated NPM1*
AML with mutated CEBPA*
AML with myelodysplasia-related changes
Therapy-related myeloid neoplasms

Acute myeloid leukaemia , Not Other Specified
AML with minimal differentiation
AML without maturation
AML with maturation
Acute myelomonocytic leukaemia
Acute monoblastic and monocytic leukaemia
Acute erythroid leukaemia
Acute megakaryoblastic leukaemia
Acute basophilic leukaemia
Acute panmyelosis with myelofibrosis
Myeloid sarcoma
Myeloid prolierations related to Downs syndrome
Transient abnormal myelopoiesis
Myeloid leukaemia associated with Downs syndrome
Blastic plasmacytoid dendritic cell neoplasm

Table revised from. (14) * Provisional entieties.

1.2 Molecular Pathogenesis of Acute Myeloid Leukemia

Knudson (15) proposed a two-hit hypothesis explaining the generation of the pathogenesis in AML from different genotypes. These genotypes involve the cooperation of gene rearrangements and mutations falling into two broad groups; class I mutations leading to a proliferative and survival advantage to the leukemic blasts, and class II mutations impairing differentiation. Additionally, recently a new class of leukemogenic genes comprising epigenetic regulation has been shown to play an important role in AML and suggests a deficiency of fulfilment in the two-hit hypothesis. (16, 17)

Initial leukocyte counts, co-morbidity and patient age are important risk assessment factors. However, cytogenetic changes in AML represent the most powerful prognostic factor regardless of age. (13) More than 50 % of AML cases are identified to have recurrent chromosomal rearrangements, (18) and risk stratification can be helpful in guiding the design of new therapeutic strategies. One well known characterized example is t(15;17)(q22;q21) encoding fusion of the promyeloid leukemia (PML) gene with the retinoic acid receptor α (RARα) gene. This fusion creates a hybrid protein that impairs the normal differentiation of promyelocytic cells. (19) The drug all-*trans* retinoic acid (ATRA) targets this class II mutated fusion protein directly to promote differentiation, and patients with this translocation are

therefore associated with a favorable prognosis. (20) Younger adult patients are classified according to three basic groups based on prognosis-associated cytogenetic aberrations; favorable, intermediate and adverse. Older patients with an age of 60 ≥ are frequently associated with decreasing incidence of favorable versus an increase in adverse cytogenetics. (21, 22) Cytogenetic normal AML (CN-AML) patients form the largest sub-group (40-50 %) in AML (13) but do also show a great heterogeneity of somatically acquired mutations. This group is initially associated to the intermediate group of the three cytogenetic classification groups, if no prognosis-relevant mutations are present. (13) The three most important somatic mutations, to date, with high prevalence in AML patients are Nucleophosmin 1(NPM1), CCAAT/enhancer-binding protein alpha (CEBPA), and FMS-like tyrosine kinase 3 (FLT3). (13) Mutated NPM1, when detected with wild type FLT3, and double CEBPA mutations involving N- plus C- terminal alterations, confer a favorable prognosis, whereas FLT3-internal tandem duplication (ITD) are associated with adverse outcome. (23) However, the relationship of genetic mutations with others, play a major role in leukemogenesis and their pathogenetic role. (24)

1.3 Epigenetic and proteomic deregulation in AML

1.3.1 Histone Acetylation

Epigenetic changes refer to alterations in the encoded heritable information by interplay of DNA and histone tail modifications. This enables a change of phenotype but does not involve a change in nucleotide sequence of the DNA. Consequently, epigenetic alterations are not mutations. (25) Acetylation, methylation, and phosphorylation on specific amino acids presented on N-terminal tails of the histone proteins, are the mostly studied epigenetic modulations besides ADP-ribosylation, ubiquitination, and SUMOylation. (26) Different epigenetic modulations occur during normal development leading to a more open chromatin configuration (euchromatin) making it more accessible for transcription, or compacting the chromatin (heterochromatin) restricting gene transcription. (27)

Most relevant for this thesis is epigenetic regulation by reversible histone acetylation performed by valproic acid. (3, 28) Histone acetyltransferases (HATs) catalyze the acetylation of lysine residues on the histone tails which opens up the chromatin and allows the transcription of genes involved in e.g. cell differentiation, growth arrest and apoptosis, while histone deacetylases (HDACs) repress the transcription of those genes by condensing the

chromatin through the removal of the acetyl groups. (26, 27) Mutated forms of both HATs and HDACs are generally rare within cancers but HDACs are shown to be overexpressed in leukemia. (29, 30) The HDACs are categorized into four main classes, with Class I including HDAC 1 to 3 and 8, whilst HDAC 4 to 7, 9 and 10 belong to Class II, Class IV contains HDAC 11, and sirtuins SIRT 1 to 7 are placed in Class III. (31) Normal cells are relatively resistant to HDAC inhibitors (HDACi) induced cell death compared to cancer cells. (32) VPA has not only been reported to inhibit the activity of HDAC Class I and II, but also to affect the expression of HDAC 2. Approximately 30 % of the protein expression level was reduced in murine F9 teratocarcinoma and human embryonic kidney HEK293T cells after 24 hours to 48 hours VPA exposure. (32) As HDAC and HAT activities regulate gene transcription, HDACis can prevent the aberrant down-regulation of essential genes by HDACs. (32) Thus, VPA affect differentiation, cell growth and apoptosis by its inhibition of HDACs.

1.3.2 Protein Regulation by Phosphorylation

Post-translational changes, by covalently modification of nascent polypeptides, are key mechanisms regulating functional diversity of proteins biological activity, protein localization within the cell, and their binding specificity. (30) The fraction of phosphorylated proteins is estimated to be one third of mammalian proteins, hence reducing the complexity of proteomic data and enriching the analysis. (33) There is no one-to-one correlation between the abundance of messenger RNA (mRNA) to the protein level in the cell. This is due to post-transcriptional and post-translational changes corresponding to differential splicing, editing and modifications. (34) Thus, the transcription of one gene can result into the translation of distinct proteins, and consequently, the transcriptional profiling does not provide a clear answer to the biological activity and the functional consequences of these changes alone. (35)

Phosphorylation is often an activating modulation that involves an enzyme-catalyzing reaction. (33) There are two ways by which the catalytic activity of an enzyme can be controlled; either by reversible interaction with ligands or by a covalent modification, such as phosphorylation. (36) Protein kinases drive the catalytic events leading to diverse downstream signaling. Investigations of AML patients have suggested that somatic genetic alterations and overexpressed enzymatically active proteins are the major factors driving the disease. (37) The MAP kinase/ERK kinase (MEK)-extracellular signal-regulated kinase (ERK) kinases are for example activated through phosphorylation and have been reported to be constitutively

activated in more than 50% of primary AML patients and can have pro-survival function. (38, 39) Phosphoproteomic analyses of primary AML-patients have also discovered post-translational modifications that may serve as response parameters prior to therapy. (34)

1.4 Treatment

1.4.1 Conventional Therapy for Acute Myeloid Leukemia

The mainstay of treatment for newly diagnosed AML patients includes cytotoxic drugs such as the standard therapy based on the cytotoxic antibiotics anthracyclines (usually daunorubicine) given the first three days with a seven day continuous intravenous infusion of the DNA synthesis blocking antibetabolite arabinosylcytosine (cytarabine). (6, 40) This treatment is also known as the conventional 3+7 regimen. (41) It starts with a remission induction therapy with the goal of patients to enter complete remission (CR), involving normalization of the immature blast cell count to less than 5% blasts in the bone marrow, the absence of extramedullary AML, and recovery in neutrophil and platelet counts. (42) Approximately 60-80% of AML patients younger than 60 years receiving standard induction therapy achieve CR, whereas only 50% of patients with an age above 60 receive CR. (13) Following induction therapy, the consolidation treatment intend to eliminate remaining leukemic blasts to prevent a possible relapse. Unfortunately, most patients experience relapse of the disease and a substantial proportion of patients older than 60 years are not considered eligible for intensive treatment. For example, the risk of cardiotoxicity associated with daunorubicin is one of the side effects impairing its use in elderly patients. (43) Elderly patients are rather given lower doses of cytarabine, acquire less-intensive chemotherapy as treatment with idarubicin (induces DNA strand breaks) or mitoxantrone (topoisomerase II inhibitor) as substituted for daunorubicin, or are recommended to take part in clinical trials with investigational drugs. (10, 44) Hypomethylating agents such as decitabine and azacitidine can also be offered to older AML patients. (45) Another consolidation therapy used is autologous stem cell transplantation (auto-SCT) where stem cells are collected from patient prior to chemotherapy or radiation treatment, removed for leukemic blasts at the laboratory, and re-infused following treatment. Auto-SCT is an option for younger patients with favorable and intermediate risk cytogenetics. (13) However, elderly AML patients tolerate this type of SCT less well than younger adults. (46) Allogeneic SCT (allo-SCT), from a human leukocyte antigen (HLA) matched donor, is a more common option in AML patients.

Patients of favorable risk AML are no longer suggested for allo-SCT therapy whilst the survival benefits for patients with intermediate- and adverse-risk AML, are currently being discussed. (47, 48) But finding a healthy HLA-matched sibling is less likely in elderly. Older patients rarely benefit from standard myeloablative allo-SCT, which consists of high dose chemotherapy with irreversible cytopenia followed by mandatory stem cell support, resulting in unacceptable transplant related mortality. (49) However, to reduce the procedure-related toxicities observed in elderly, conditioning with myeloablative alkylating agents and fluarabine have been introduced giving improved results without negotiating the efficacy of the transplant. (50)

1.4.2 Valproic Acid in the Treatment of Elderly Patients

Therapy designed for older AML patients has not improved in recent years compared with the considerable progress made in younger patients (51) and the options available are variations of standard therapy , treatment by investigating agents in clinical trials or palliative care. But as they cannot receive the standard therapy due to an unacceptable risk of mortality, less intensive strategies are coveted.

Valproic acid is a well-tolerated antiepileptic drug that is competent in inducing apoptosis and myeloid differentiation in AML. (52) Studies performed on other low toxic chemotherapy combined with VPA, e.g. ATRA, decitabine and 5-azacitidine, report toxicity effects to be acceptable in older patients with VPA, and to alter the sensitivity of the agents to AML. (53, 54) Induction of chemosensitivity is observed when VPA is combined with the cytotoxic drugs 6-mercaptopurine (6-MP) and hydroxyurea (HU). (55) HU and 6-MP are already well established agents and their combination have shown to stabilize AML in relapsed patients. (56-58)

Nevertheless, complete hematological remission is uncommon and only 20-30% of patients respond to VPA by showing disease stabilizing effects. On the other hand VPA affects the peripheral blood cells composition by increasing the platelet count. And as thrombocytopenia (abnormally low levels of platelets in blood) is a common side effect of chemotherapy, VPAs increasing platelet count is encouraging concerning blood transfusion independence. (52)

1.4.3 The Molecular Potential and Toxicity of Valproic Acid

VPA (2-propypentanoic acid) is a branched short-chain fatty acid, naturally produced by the plant *Valeriana officinalis*, and synthesized as an organic solvent by B. S. Burton in 1882. (59) It is one of the most widely prescribed antiepileptic drugs, also used in the treatment of bipolar disorder, and associated with few side effects. However, VPA is known to be teratogenic when used during early pregnancy, restricting its use in pregnant women. (59) It selectively targets the HDAC class I and less strongly HDAC class II, through inhibition. (60) HDAC Class II are fundamental transcriptional regulators of several developmental and differentiation processes (32) whereas HDAC Class I play an important role in proliferation and cell survival. (61) As they both repress transcription, VPA has shown to reactivate the abnormal repressed proteins that have been shown to be important tumor suppressors, for example expression reactivation of E-cadherin, $P21^{CIP1}$. (30) One indirect target of VPA is $p21^{WAF1}$/CDKN1A, a cyclin dependent kinase associated with cell cycle arrest in G1/S phase. (62) This increase of p21 protein expression does not appear to be dependent on the tumor suppressor p53, also known as the guardian of the genome. p21 alters molecular pathways which in this case would generally lead to cell cycle arrest and apoptosis.

Active signaling pathways in AML after a response by VPA treatment was investigated in the Brown Norwegian Myeloid Leukemia (BNML) rat model, and the discovery of novel resistance pathways of VPA was facilitated by the project supervisor Rakel B. Forthun and her colleagues. (3)

1.5 Phosphoprotein Expression Analysis in Acute Myeloid Leukemia

1.5.1 HK1 and HPRT1 are regulated by Valproic Acid in the BNML Rat Model

As described above, VPA is effective in the treatment of a subgroup of AML patients. As the capacity of cells to maintain cellular survival networks may determine their fate of survival, phosphoprotein expression was investigated in the BNML rat model. The BNML model is a syngeneic model of human AML, and exhibits many properties that are common with those of human AML patients, including an intact immune system. (63, 64) The BNML rats are highly responsive to treatment with VPA and can be used to investigate response mechanisms of this drug. To elucidate which networks that might contribute to survival of AML cells after exposure to VPA, animals were treated for four weeks, and leukemic cells were harvested from the spleens when the rats were at a clinical endpoint. (3, 65) Immobilized metal affinity chromatography (IMAC) enrichment was used to purify the phosphoproteome before co-

detection and quantification through fluorescent labeling by difference gel electrophoresis (DIGE) and identified by mass spectrometry. Twenty-one novel phosphoproteins were discovered to be modulated by VPA, and the researchers suggested that targeting these proteins with small molecular inhibitors in combination with VPA could possibly increase the anti-leukemic effect of VPA. Hexokinase 1 (HK1) and hypoxanthine – guanine phosphoribosyltransferase 1 (HPRT1) were two of the differentially expressed phosphoproteins that were identified in this study. The remaining phosphoproteins will not be covered in this thesis. Both phosphoproteins were found to have reduced expression after treatment with VPA. HK1 is a direct target of Lonidamine (LND), whereas the signaling pathway of HPRT1 may be targeted by Mycophenolate mofetil (MMF). Both proteins and drugs will be described further in the next chapters.

1.5.2 Deregulation of Metabolism during Tumorigenesis

The metabolic effect of HK1 and HPRT1 will not be covered in depth in this thesis, but will be briefly described in the following section.

Tumor cells are known to have a high metabolic state. (66) This is done by increasing the energy production through the synthesis of lipids, proteins and nucleotides in a manner conducive to proliferation. (67) Most biological energy is normally driven from oxidation of reduced metabolites (respiration). Even though there is an adequate presence of oxygen, cancer cells tend to shift their energy metabolism from primarily relying on mitochondrial oxidative phosphorylation, towards a more ineffective way of producing energy by large amounts of lactate, referred to as aerobic glycolysis. (68) This phenomenon is called The Warburg effect. (69) Why and how cancer cells use this to their advantage is uncertain, and how this can be utilized to an advantage of representing potential targets for therapeutic intervention is widely focused on in recent research. (70) The two enzymes investigated in this thesis HK1 and HPRT1, are both involved in the processing of two important energy sources in cancers; glucose and glutamine. Transformed cells consume large amounts of glucose entering the cell by plasma membrane glucose transporter (Glut) and captured by hexokinase for the stimulation of downstream reactions of glycolysis. (71) The glycolysis is held intracellular of the cytosol and can either proceed via the citric acid cycle under aerobic conditions inside the matrix of mitochondria, or under anaerobic conditions to produce lactate. (72) Glutamine is known to be a key supplement in the culture medium supporting cancer growth and it can be metabolized and drive energy production of the TCA cycle in

mitochondria to produce adenosine triphosphate (ATP) in a glucose independent manner and function as a precursor for the synthesis of lipids, proteins, and nucleotides. (73)

1.5.3 Hexokinases

Hexokinases phosphorylate 6-carbon sugars using Mg-ATP as phosphate donor, of which glucose is the major hexose for most cells to produce energy via glycolysis. (36) Four different isoforms of hexokinases exist in mammalian tissues; HK 1-4. (74) Their distinct kinetics distinguished their main tissue specificity. Hence, HK4 is mainly found in the liver having low affinity for glucose, whilst HK3 is found in the erythrocytes and is least abundant in the body. (75) HK1 is the major isoform found in erythrocytes and in the brain with highest affinity for glucose, and together with HK2 the main isozymes in muscle. HK2 has high affinity to glucose and has a higher enzymatic activity than the other isozymes. (70, 76) The higher activity of HK2 might be explained by the two catalytic sites it consists at the C-terminal and the N-terminal domain. (74) In contrast only the C-terminal has catalytic activity in HK1 and HK3. (75) HK4 is smaller than the other hexokinases and is not inhibited by its own product glucose-6-phosphate (glucose-6-P) which HK1-3 are. However, the presence of inorganic phosphate antagonizes the inhibition of only HK1 by physiological glucose-6-P. (76) But to facilitate enzymatic activity for catabolism of glucose, HK1 and HK2 need to be associated with mitochondria. HK2 is suggested to be subcellular translocated for anabolic uses. (77) At mitochondria localization, HK1 and HK2 are associated to the voltage dependent anion channel (VDAC) through the N-terminal peptide of both isozymes, facilitating a directly interaction of the intra-mitochondrial ATP synthesis to glucose metabolism. (66) HK3 lacks this sequence of the N-terminal, thus is not bound to mitochondria. (66) This first committed step of glucose metabolism plays a role in generating energy by converting glucose to the final product pyruvate and ATP, and metabolic intermediates such as lipids and nucleotides, for other pathways. (66) The binding of HK1 and HK2 to VDAC reduces the available sites for pro-apoptotic factors such as Bak and Bax, thus playing a role in preventing tumor apoptosis. (70) Interestingly, attention has been brought to HK1 and HK2 as they have been shown with an elevated activity in cancer cells being less predisposed to inhibition by their product glucose 6-phosphate allows. (70, 78) The up-regulation of HK2 was reported to protect leukemic cells from cell death by escaping the intrinsic apoptosis signaling pathway. However its dissociation from the mitochondria resulted in induction of apoptosis in HL60 AML cells. (70, 79) Inhibition of this step by an

inhibitor may limit the possibilities of cancer cells to regulate the glycolytic pathway, for example by their production of higher amounts of lactate. Phosphofructokinase and pyruvate kinase serve as the key regulatory targets of glycolysis, and the selective switch to an isoform of the pyruvate kinase, PK-M2, has been suggested to be upregulated in leukemia. (80, 81) Thus, targeting a catalyst early in the glycolysis pathway may hinders the build-up of downstream effects such as PK-M2, or the flux of metabolic intermediates that could be shunted into other biosynthetic pathways to the advantage of cancer cells. (36) This might, in turn, shift the energy production from glycolysis to cellular respiration in a mitochondria dependent citric acid cycle manner. Combining another drug targeting HK1, that could lead to a reverse of the enzyme`s anti-apoptotic effect, together with VPA may increase its sensitivity to AML cells having elevated glycolytic activity, thus increasing responsiveness of patients.
The expression of phosphorylated HK1 was found to be reduced after VPA treatment in BNML rats. (3) Since this was discovered in late stage disease animals, further analysis was needed to unravel whether the reduction was an anti-leukemic effect by VPA or a resistance mechanism to VPA.

1.5.4 HPRT1

Nucleotide biosynthesis is essential for cancer cells to divide. (82) The nucleotide pool has been revealed to be larger and the activity of the anabolic pathway is preferentially high in rapid proliferating cells. (5, 83) The purine nucleotides include adenine and
guanine where their respective nucleotide triphosphates, ATP and GTP, are active in the metabolism. The synthesis of nucleotides can arise through *de novo* synthesis or through the *salvage pathway* in a glutamine-dependent manner. (71) In both pathways inosine 5`-monophosphate (IMP) is a branch point between guanine and adenine nucleotides, and it is the first fully formed purine nucleotide **(Figure. 1)**. During the *salvage pathway*, this compound derives from the purine base hypoxanthine. Hypoxanthine guanine phosphoribosyl transferase (HGPRT) catalyzes this reaction to guanosine monophosphate (GMP). Inosine monophosphate dehydrogenase (IMPDH) converts IMP to xathosine monophosphate (XMP), which is subsequently catalyzed to GMP by GMP synthetase (GMPS). An alternative way of the *salvage pathway* is the directly conversion of guanine to guanosine monophosphate led by HGPRT. (84) The production of IMP in the *de novo* synthesis pathway uses seven ATPs. (85) The *de novo* pathway, which is essentially identical in all organisms, is an energy-consuming pathway which replicating hematopoietic cells are greatly dependent on. (86) The *salvage*

pathway utilizes bases or nucleosides available through enzymatic breakdown of DNA and RNA or which become available through diet. (36) HPRT1 encodes the enzyme HGPRT which adds an activated ribose-5-phosphate to bases, thereby re-utilizing the free bases by creating nucleotides through the *salvage pathway*, as previously shown by **Figure 1**. IMPDH catalyzes the rate-limiting step within the complex biosynthesis of *de novo* guanosine nucleotides. Studies report an elevated level of IMPDH activity in AML patients and the two isoforms of the dehydrogenase (IMPDH1/2) in peripheral blood mononuclear cells (PBMC) have also been investigated. (87) Implications of a high expression level of type I mRNA in PBMCs and lower expression of the type II mRNA of IMPDH in PBMCs were made. (88) The opposite has been reported in leukemic cells where activity of IMPDH type II at both the mRNA and protein expression level, were higher than that of lymphocytes. (89) Densitometric analysis on Northern blots performed on the expression level of IMPDH in two AML patients in the study mentioned above, suggested type II mRNA to be the main isoform resulting in an increase of a total IMPDH activity in leukemic cells. (90) Goldstein and co-workers report the induction of myeloid differentiation in HL60 cells after tiazofurin treatment, whose mechanism of action is known to be inhibition of IMPDH. (90) Further analysis needs to explore whether cancer cells use the *salvage pathway* to circumvent a block in the *de novo* purine pathway when exposed to chemotherapeutic agents targeting IMPDH.

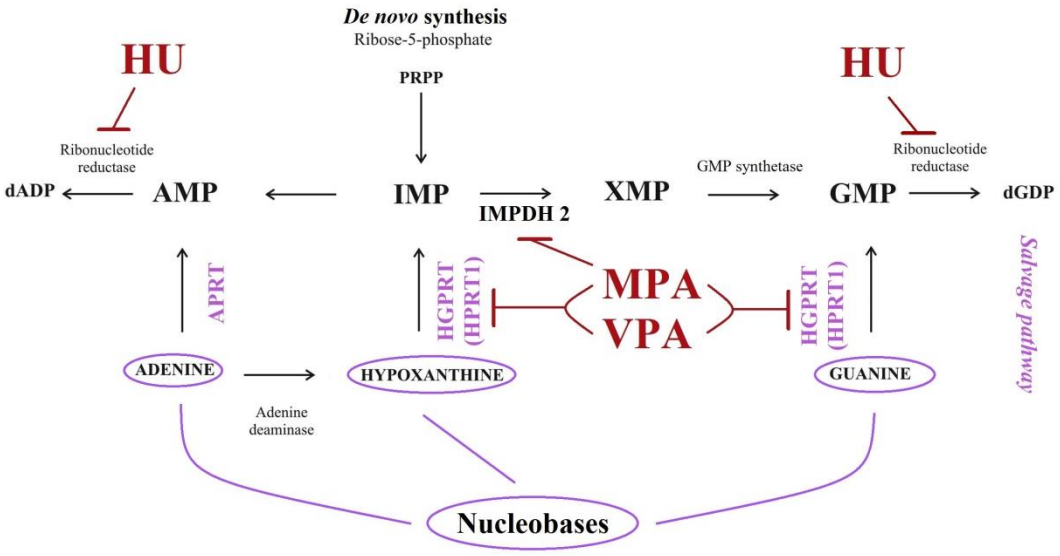

Figure 1. Hypothetic drug influence on Purine nucleotide metabolism. Reuse of purine bases involves the *salvage pathway* and the *de novo* synthesis of purine from ribose – 5 – phosphate precursors. The HGPRT signaling pathway inhibitor MPA and VPA may influence the synthesis of purine nucleotides through the *salvage pathway*, and IMPDH 2 converting IMP to XMP in the *de novo* pathway is inhibited by MPA. Hydroxyurea (HU) inhibits ribonucleotide reductase converting purine

nucleotides (AMP, GMP) into purine deoxyribonucleotides (dADP, dGDP). Figure was revised from (91).

1.6 Mycophenolate Mofetil as a potential anti-leukemic agent

Mycophenolate mofetil (MMF) is approved for its use as an immunosuppressant agent in the prevention of organ transplant rejection by holding lymphocyte-selective anti-proliferative effects. (92) Several different chemical syntheses of the phenolic acid have been explored to increase its bioavailability since its initial purification from a *Penicillium* species grown in deteriorated maize in 1893. (93) Gosio *et.al.* found that the active compound, mycophenolic acid (MPA), exerted an antifungal property. Nonetheless, MMF exhibits attributes as a reversible and noncompetitive inhibitor of IMPDH controlling the *de novo* guanosine nucleotide pool synthesis. There exists two human isoforms IMPDH1 and IMPDH2 that are closely related but encoded from two different genes. (93) Lesch-Nyhan syndrome is characterized by a lack of HPRT1 gene, thus are not able to recycle purines through the *salvage pathway*. However, reports show affected people with this syndrome having essentially normal function of T- and B-lymphocytes. (94) This lead to the discovery of proliferating lymphocytes being depending on *de novo* nucleotide synthesis for mitogenic and antigenic stimulation. (95) Interestingly, a fivefold of inhibition potential of MPA on type 2 IMPDH has been reported, which has been found to be the main isoform in leukemic cells. (87) Synergistic effect has been reported in CML cell lines, where the combination of MMF and imatinib overcome the initial resistance to tyrosine inhibition kinase inhibition (TK1). (96) Induction of differentiation of HL60 and K562 leukemic cell lines has been shown after treatment with MPA. (97) These observations, among others, make MMF to an interesting agent for further investigation of the anti-leukemic effect by targeting the purine biosynthetic pathway in AML cells. As explained by **Figure 1**, the inhibition of IMPDH by MMF involves the same purine nucleotide synthesis only downstream of the catalyst HGPRT to where VPA has been suggested to provoke an effect. Thus, the remaining alternative to produce GMP after IMPDH inhibition is through the alternative enzymatic activity of HGPRT which does not involve the conversion of IMP to XMP but a direct conversion of guanosine to GMP. Thus the anti-proliferative effect seen of VPA might be potentiated through the combination with MMF.

1.7 Lonidamine

The effect the indazole carboxylic acid derivative Lonidamine (LND) as an anti-spermatogentic agent and on embryotoxicity was already clarified in the early 1980. (98) Nevertheless it was soon found to bind to mitochondrial bound hexokinase and inhibit its action. (99) Further interpretations based on experiments with the drug suggest its activity to be membrane-associated rather than direct on the enzyme itself. (98) LND selectively inhibits mitochondrial bound hexokinase and not cytosolic hexokinase, and is suggested to result in a distinct effect on glycolysis in normal versus neoplastic cells. LND evokes a decrease in oxygen consumption in both cancer and normal cells, but enhances aerobic glycolysis in normal cells while it inhibits both aerobic and anaerobic glycolysis in human cancer cells. (100) Activation of mitochondrial hexokinases is shown to be regulated by Akt/PKB-mediated phosphorylation. (101) As already mentioned in previous chapters, activated mutations of kinases within ERK signaling pathways are frequent events in tumors and also in leukemia. ERK and the signaling protein AKT usually operate to negatively regulate apoptosis induction. (102) Previous studies report a suppressed efficacy of LND on leukemic cells *in vitro* which provoked an activation of this defensive pathway. (103) However, attenuating this activation potentiated LND. VPA has been reported to increase the expression of phosphorylated ERK. (104) If LND and VPA work in tandem, the suppressed drug effect by this pathway may be withdrawn.

LND possesses poor clinical efficacy when used alone for its anti-tumor properties, however it is suggested to sensitize cells to other drugs when combined with for example DNA-damaging chemotherapeutics. (105) It might also possess a property to overcome multidrug resistance by inhibiting cell recovery from potentially lethal damage. (103, 106) Its clinical value and efficacy has been proved in combination treatment in completed phase III trials and several studies advanced ovarian cancer, (107) glioblastoma multiforme, (108) metastatic breast cancer, (109) and inoperable non-small lung carcinoma. (110) Previous *in vitro* studies on leukemic cell lines have included LND for the investigation of its anti-leukemic effect in cooperation with the drugs Etomoxir, Arsenic trioxide (ATO), cisplatin and curcumin. (111, 112) Etomoxir and LND worked together by inducing apoptosis of HL60 cells whereas curcumin seemed to potentiate the toxicity of both LND and ATO by generating reactive oxygen species (ROS). (4)

2. Aims

The potential of VPA was demonstrated by an increase of survival in the rat leukemia model BNML. HK1 and HPRT1 are two proteins found to be up-regulated in AML patients, and down-regulated in VPA treated BNML rats. However, since the leukemic cells were harvested when the rats were sacrificed at humane endpoint, it is of interest to explore whether the proteins were regulated as an anti-leukemic effect or a resistance mechanism to VPA by the leukemic cells. In this aspect we wish to use the AML cell lines HL60, MOLM13 and NB4 to:

1. Explore the effect of HK1 inhibitor LND and HPRT1 signaling pathway inhibitor MMF in regulating cell death investigating morphological changes by Hoechst 33342 and phosphoserine membrane alteration and cell permeability by Annexin-V/PI flow cytometry, and metabolic activity by WST-1 assay

2. Investigate the effect of MMF, LND and VPA in activating proteins involved in apoptosis (caspase 8 and 9), cell cycle (p21), proliferation (ERK1/2) through Western blotting

3. Evaluate whether VPA shows synergistic anti-leukemic effect when combined with MMF or LND using the method mentioned in aim 1, or transient knockdown by siRNA to HK1 or HPRT1

3. Materials and Methods

3.1 Cell culture

3.1.1 Culturing cells

The human acute myeloid leukemia (AML) cell lines MOLM-13, HL60 and NB4 are convenient *in vitro* tools for chemotherapeutic and pharmacologic investigation and they may provide a good basis for studies aiming to understand the control of e.g. the differentiation in AML. (113) The use of AML cell lines in experiments allows for comparison to other studies. MOLM-13 carries an internal tandem duplication of the FLT3 gene with a functional TP53 that resembles the majority of primary AML patients. (114) The genetic aberration provides the cell a survival and proliferative advantage. HL60 exhibits a deletion of TP53 gene but carries an intact FLT3, whereas NB4 is a human acute promyelocytic leukemia (APL) cell line with t(15;17), also carrying a mutated TP53. (115, 116) The three AML cell lines were selected to represent the varying genotypes of some patient subgroups found in the heterogeneous disease.

All cell lines were grown in Roswell Park Memorial Institute (RPMI) - 1640 medium (Sigma-Aldrich, Inc. St. Louis, MO, USA) supplemented with 10% heat inactivated Fetal Bovine Serum (FBS), 1% Penicillin /Streptomycin (PS) (Sigma-Aldrich) and 1% L-glutamine (LG) (Sigma-Aldrich). The cells were incubated and kept at 37 ºC in a 5% humidified atmosphere incubator and split every second day. All three cell lines are spherical in shape and grown floating in the culture medium (suspension culture). Personal protective equipment was worn when working with cell cultures in a cell culture hood, providing an aseptic work area. The cells in suspension were passaged before they had clumped together and reached confluence. HL60 tend to form clusters although they have not reached confluence. The cell lines were passaged every second day by withdrawing of a portion of cells from the culture flask and diluted down to the appropriate seeding density. Prior to this, cells were counted by using the Bürker chamber. Ten µL cell suspensions were applied to the chamber (0.1 mm) before counting the cells in three subsequent squares. The number of cells was divided by three to get the average of cells in million per mL cultivated cell suspension.

HL60 was maintained between 0.5-1.0×10^6 cells/mL in a split ratio at 1:5 to 1:6, MOLM13 to 1:4 to 1:5 at about 0.6-1.5×10^6 cells/mL, while NB4 cells were maintained between 0.5-1.0×10^6 cells/mL and split at 1:4.

3.1.2 Cell thawing

Cryopreserved (10% dimethyl sulfoxide (DMSO, Applichem Panreac, GmbH Darmstadt, Germany)) cell aliquots were retrieved from liquid nitrogen storage, thawed until a small bit of ice remained in the vial and supplied 800 µL of complete fresh growth media (RPMI 1640, 20% FBS, 1% PS, 1% LG). After five minutes incubation in at RT, the cell suspension was mixed gently by pipetting. The cell suspension was transferred to 15 mL tubes containing 5 mL complete media and centrifuged at 1200 rpm for 5 minutes at RT, with break. The supernatant containing fragmented cells and cryoprotectant was removed before resuspending the pellet containing viable cells in 7 mL medium and transferred to a cell culture flask of 25 cm^2. If a large degree of cell debris was observed the following day, the cells were centrifuged and resuspended in new complete media.

3.1.3 Cryopreserving cells

Fresh complete media was added to cell cultures the day before cell aliquots were frozen for long time storage. Cells were counted and 5×10^6 cells were harvested by centrifugation at 1200 rpm for 5 min at RT, with break. Freezing medium was added the pellet (70% complete RPMI 1640, 20% FBS, 10% DMSO). Cryovials (Sarstedt, Nümbrecht, Germany) containing 1 mL of cell suspension were placed in a polystyrene box to decreasing the temperature approximately 1 ºC per minute at -80ºC until they have reached the equivalent temperature, then transferred to a liquid nitrogen tank (-196ºC). (117)

3.2 NOD/scidILrgamma mice model

NOD/scidILrgamma (NSG) mice, double homozygous for the severe combined immunodeficiency mice, (118) were bred in the Laboratory Animal Facility Vivarium at the University of Bergen accredited by Association for Assessment and Accreditation of Laboratory Animal Care (AAALAC) International. The mice were originally provided as a gift from Leonard Schults (Jackson Laboratory, USA). Their care and housing were in accordance with institutional guidelines. (119) Animals were maintained in specific pathogen-free conditions by housing in closed, internally ventilated cages (IVC), and by conducting work in a clean manner by following the dress code of complete change of clothing, wearing mask, gloves, separate shoes and a coat. A Maximum Tolerated Dose (MTD) pilot study was performed on three female NSG, 8 weeks old, mice by giving 25 mg/kg, and 50 mg/kg Lonidamine (LND, AbMole Bio Science, CAS No.: 50264-69-2) dissolved in 70%

Poly(ethylene glycol) (PEG300) (Sigma Aldrich), 20% ddH_2O and 10% DMSO, resulting in reproducible injection of the compound. Intraperitoneal injection (i.p.) was used to administer the drug once a day. Two male NSG mice, 18 weeks old, received the drug vehicle only (70% PEG300, 20% ddH_2O, 10% DMSO). Doses were selected based on previous performed *in vivo* studies and duration of dosing depended on parameters such as clinical signs, weight loss and food consumption. (120) The pilot study was designed to minimize the number of animals by injecting NaCl subcutaneous over the shoulders, into the loose skin over the neck, to recover from treatment if necessary by signs of dehydration and weight loss.

3.3 Drugs

Lonidamine (Sigma Aldrich, lot# 043M4038V, and CAYMAN Chemical company, item: 14640), Lonidamine (AbMole BioScience, CAS No.: 50264-69-2) and 6-Mercaptopurine monohydrate (Aldrich Chemistry, CAS: 6112-76-1) were dissolved in DMSO, at 100 mM and stored at -20 ºC. Mycophenolate mofetil (CellCept) (90 mM) was dissolved in DMSO and stored at -80ºC. Hydroxyurea (Sigma Aldrich, H8527) was solved in 1xphosphate buffered saline (PBS). Sodium valproate (DESTIN Pharma, item: 04 69 87, Germany) obtained as injection fluid was stored at 4 ºC. All drugs were freshly prepared from stock solutions for each experiment. For experiments on drugs when DMSO was used as solvent in in vitro studies, concentrations of less than 1% (v/v) DMSO have been shown to not interfere with the results. (121) The negative controls in this thesis did not exceed 0.5% DMSO.

3.4 Cell proliferation assay

Spectrophotometric quantification of cell proliferation was assayed by the water soluble tetrazolium salt-1 (WST-1) (Roche Ltd, Basel, Switzerland) based colorimetric assay. This tetrazolium salt is reduced extracellularly to formazan dye by enzymes of the plasma membrane oxidoreductase. (122) The primary reductant is NADH derived from the TCA of the mitochondria. Hence, WST-1 is converted by metabolically active cells and was employed to measure cell proliferation. The cell lines HL60, MOLM13 and NB4 were plated in triplicate (20×10^3 cells/well) in a 96-well microplate and treated with either LND (1, 5, 20, 50, 100, 200, and 500 µM) or MMF (0.01, 0.25, 0.5, 1.0, and 2.5 µM) or in combinations with Valproic acid (0.05 mM – 2.5 mM), Hydroxyurea (2, 10, 40, 100, and 200 µM), 6-Mercaptopurine monohydrate (1, 5, 20, 50, and 100 µM) in fixed ratios, to a final volume of 100 µL/well. The negative control contained 90 µL cell suspension and DMSO (vehicle)

(v/v%). Following the drug exposure and cell incubation at 37ºC and 5% CO_2, Cell Proliferation Reagent WST-1was applied to all wells with a final dilution of 1:10 two hours prior to examination of the cells after 24 hours or 48 hours treatment. The absorbance was measured at a wavelength of 450 nm, with a reference wavelength of 620 nm using the Spectramac Plus 348 Spectrophotometer (Molecular Devices Corp., Sunnvale, CA, USA). Background absorbance was removed by subtracting values obtained from wells containing no cells. The spectrophotometer automatically subtracted the absorbance measured of the reference wavelength from that measured from the current wavelength. The value obtained from the blank (complete medium only) was subtracted manually from all wells before they were normalized to the negative control prior to calculating the percentage metabolism in each well, followed by this formula:

$$\left(\frac{Arbitrary\ units\ (AU) of\ treated\ sample}{AU\ of\ negative\ control}\right) x\ 100$$

Native human AML patient blasts derived from the peripheral blood were separated by density gradient (1.077 g/mL, widely used) at the laboratory resulting in AML blast population purity of higher than 95%. (113) Two different patient samples were obtained at the time of diagnosis. One consisted of peripheral blood sample only whilst both bone marrow and peripheral blood samples were provided from the second AML patient. As defined by WHO, at least 20% of the bone marrow or blood of AML patients is required to include leukemic blasts. The high blast count in the peripheral blood is only seen in subgroups of patients. (113) The patient samples were diluted in Iscove`s Modified Dulbecco`s Media (IMDM) containing 20% heat inactivated FBS, 1% LG and 1% PS, counted and plated in triplicate (1×10^6 cells/mL) in a 96-well microplate and treated with LND (5, 10, 20, 50, and 100 µM) alone and in combination with VPA (0.05, 0.1, 0.2, 0.5, and 1 mM), and with MMF (0.1, 0.25,0.5, 1, and 2.5 µM) alone and in combination with VPA (0.1, 0.25, 0.5, 1, and 2.5 µM) to a final volume of 100 µL/well. WST-1 was added to all wells (1:10 final dilution) two hours prior to spectrophotometric analysis of the cells after 48 hours treatment, examined similar to the cell lines above.

Cryopreserved (10% DMSO) PBMCs were resuspended in IMDM supplemented with 20% FBS, 1% LG and 1% PS, counted and diluted into 1×10^6 cells/mL and incubated for 1 hour at 37 ºC in a 5% humidified atmosphere incubator prior to further experiments. Single-drug treatment by 48 hours consisted of LND (5, 10, 20, 50, 100, 200, and 500 µM) and MMF (0.1,

0.25, 0.5, 1, and 2.5 µM) to a final volume of 100 µL/well. Two hours prior to examination by spectrophotometer, the reagent WST-1 was applied in a final dilution of 1:10.

3.5 Cell viability assay

3.5.1 Nuclear morphology assay

The nucleic acid staining reagent Hoechst was used to construct a visible parameter for the discrimination of normal from abnormal nuclei. The cell fixation and staining solution contained 8% Formaldehyde (Merck-Chemicals KGaA, Darmstadt, Germany) diluted in sterile phosphate buffered saline (PBS), and Hoechst 33342 DNA stain (20 µg/mL) (Calbiochem, Merck KGaA, Darmstadt, Germany). Immediately after measurement of proliferation as described above, Hoechst dye solution was added to the 96-well plates in a ratio of 1:1 (v/v) and incubated for 1 hour (4 ºC) prior to analysis of nuclear morphology using a Leica DM IRB fluorescence microscope. Cells were scored as normal or abnormal where abnormal nuclear morphology was defined as fragmented nucleus and hyper condensed chromatin morphological changes characteristic for apoptosis. (123) Cells without these characters were scored as normal. For each well, approximately 300 cells were counted to calculate the percentage of normal versus abnormal nuclei at each treatment dose. Nucleus staining images were obtained using DAPI filter. Percentage of normal nucleated cells were normalized to negative control containing cells added vehicle (0.025 % DMSO) and plotted against concentrations into a grouped graph using GraphPad Prism 6.0.

3.5.2 Annexin-V/PI Flow cytometry- Phosphatidylserine exposure

A surface change common by many apoptotic cells is a naturally flip of phosphatidylserines (PS) from facing the cytosolic side of the cell membrane to being exposed on the outer leaflet of the plasma membrane. (124) This is one of the earliest indicators of apoptosis which can be studied by Annexin V`s high affinity for this negatively charged phospholipid. Annexin V is not membrane permeable and can therefore be utilized by flow cytometric analysis to recognize apoptotic cells when conjugated to a fluorochrome. (125) Cells were plated at a density of 0.2×10^6 cells/well in a 24-well plate and treated with LND (1, 5, 20, 50, 100, and 500 µM), VPA (0.05, 0.1, 0.2, 0.5, and 1 mM) alone and in combination, or with MMF (0.1, 0.25, 0.5, 1.0, and 2.5 µM), VPA (0.1, 0.25, 0.5, 1.0, and 2.5 mM) alone and in combination, to a final volume of 1 mL in each well for 48 hours at 37 ºC and 5% CO_2. Hundred microliter of cell suspension from each sample was stained with Hoechst and put aside as an additional

control of viability. A volume according to 200 000 cells was transferred to a flow tube and washed with 1 mL 0.9% ice-cold NaCl and pelleted through centrifugation at 1000 rpm, 5 minutes, RT. Each sample was resuspended in 50 µl 1x Annexin V Binding Buffer (BB) (Invitrogen, Carlsbard, CA, USA) and 2 µL fluorescent Alexa Fluor® 647-conjugated Annexin V (catalog number: A23204, Molecular Probe, Thermo Fisher Scientific Brand). Five thousand cell events were collected for each sample on the Guava EasyCyte Flow Cytometer containing a dual laser (blue 488 nm, red 640 nm) configuration (6-2L & 6HT-2L System Optical Layout). Samples were kept on ice for approximately 15 minutes before 200 µL 1xAnnexin V BB/propidium iodine (PI) was added to ~ 100 000 cells prior to analysis. Late apoptotic and necrotic cells are permeable to PI whilst viable cells exclude this vital dye. (125) Visible light emitted by Alexa647/Annexin V was captured by the Red2 Fluorescence channel (bandpass filter (661/19)), and PI by the yellow channel (bandpass filter (583/26)). A negative control was included containing both fluorophores and cells in the absence of the inducing agent (LND, VPA, MMF) and positive controls containing the highest concentrations of drug resulting in a suspected positive value of cell death (500 µM LND, or 7.5 µM MMF).

3.6 Phosphoprotein purification from Cultured Cells

Affinity chromatography was used to separate phosphorylated from non-phosphorylated cellular proteins. The phosphate groups on amino acids carried by proteins were specifically retained on the resin within the columns, whereas proteins lacking phosphate groups were discarded in the flow-through fraction. This in situ phosphorylation procedure was based on the manufacturer` s instruction (QIAGEN). (126) All reagents used were provided by the manufacturer (QIAGEN GmbH, Hilden, Germany, cat. No.37101). HL60, MOLM13 and NB4 cell suspensions of 10^7 cells in 20 mL complete medium per cell culture flask (75 cm^2) were treated with 1 mM Valproic Acid and incubated for 48 hours in a 37 ºC humid CO_2 incubator. Ten million cells were harvested by centrifugation, 1500 rpm, 6 min, 4 ºC and lysed in 5 ml of Phosphoprotein Lysis Buffer (25 mM 2-Morpholino-ethanesulfonic acid monohydrate (MES), 1 M NaCl, 0.25% [w/v] CHAPS, pH 6.0) containing one protease inhibitor tablet and 10 µL Benzonase® Nuclease (DNase/RNase, > 99% purity) vortexed briefly every 10 minutes for 30 minutes at 4ºC. (126) The protein supernatant was harvested after centrifugation (13 000 rpm, 4ºC 30 minutes) and concentration was determined by the Bradford method as previously described. Two point five mg of total protein was adjusted to

0.1 mg/mL with the Phosphoprotein Lysis Buffer and added to the separation columns after equilibration of the columns. To generate a flow rate of approximately 0.5 mL/min for optimal binding, half of the lysate was poured into the column and allowed to enter the gel bed of the column before applying the second half of the lysate. Columns were washed once with PhosphoProtein Lysis Buffer (0.25% CHAPS) before collecting the phosphorylated proteins using the PhosphoProtein Elution Buffer (50 mM Potassium phosphate, 50 mM NaCl, pH 7.5, 0.25% CHAPS). The protein fractions were concentrated by applying 500 µL of phosphorylated protein eluates into NanoSep Ultrafiltration Columns, centrifuged for 10 min., 13 000 rpm, and combined into one column prior to protein concentration determination. Samples were stored at -80 ºC.

3.7 Isolation and quantification of cellular proteins

The cell lines HL60, MOLM13 and NB4 were counted and diluted into cell culture flasks (10×10^6 cells per flask), treated with 100 µM LND, 1 mM VPA, and in combination for 48 hours and incubated at 37ºC with 5% CO_2. Cells were centrifuged at 1500 rpm for 6 minutes, 4 ºC. The pellet was washed three times in ice cold 0.9% NaCl before lysing the cell pellet in SHIEH Lysis Buffer (10mM Tris pH 7.5, 1 mM EDTA, 400 mM dithiothreitol (DTT), Complete Mini Protease Inhibitor Cocktail (Boeringer Mannheim), and Phosphatase Inhibitor Cocktail tablet). The cell lysate samples were homogenized by gentle pipetting and kept on ice for 30 min before centrifugation for 30 minutes at 13 000 rpm, 4ºC. The supernatant, containing cell lysate, was harvested and stored in -80ºC until use.

Protein concentrations were determined using the Bradford method. (127) In brief, six different standard samples containing Quick Start Bradford 1x Dye Reagent (Bio-Rad Laboratories, Inc. US) and Bovine serum albumin (BSA) (Roche Diagnostic GmbH, Mannheim, Germany) in a linear range of 0-10 µg/mL were constructed. Protein samples to be analyzed were diluted 1:1000 with Bradford solution, before samples and standards were investigated at 595 nm using a microplate reader. The protein solutions were assayed in triplicates and normalized to the blank sample containing dye reagent only. A standard curve was created by plotting the absorbance of the standard samples on the y-axis, against the standard concentrations on the x-axis, obtaining a point-to point relationship for this set of standards. A best-fit linear regression line of the entire standard points resulted in an equation formatted as following:

$Y = ax^2 + bx + c$, where solving for x was used for interpolating the test sample concentrations. The linear regression (R^2) coefficient indicated how well the obtained data fitted to the line.

3.8 Antibodies

3.8.1 Primary antibodies

Rabbit polyclonal antibody to GAPDH 100 µg (1mg/mL, cat. no. ab9585) and Rb pAb to coxIV (1mg/mL, cat. no. ab16056) provided by Abcam were used as loading controls for western blotting. Other antibodies for target proteins used were rabbit polyclonal IgG antibody to caspase-8 p20 (H-134, cat. no. sc-7890), rabbit polyclonal antibody to caspase-9 p10 (cat. no. sc-7885), rabbit polyclonal anti-pERK (Thr202/Tyr204) (Lot # G2513) and mouse polyclonal antibody ß-actin (C4, cat. no. sc-47778). These primary antibodies were all ordered from the supplier Santa Cruz Biotechnology whereas the mouse mAb to p21 ([EA 10], ab16767) was provided by Abcam®, and monoclonal Anti-p21/WAF1/Cip1 (clone P74) was gotten from EMD Millipore. The mouse monoclonal Anti-HK2 antibody (SAB5300278) was ordered from SIGMA-Aldrich Life Science.

3.8.2 Secondary antibodies

Rabbit anti-HRP Ab and Peroxidase-conjugated AffiniPure Donkey Anti-Mouse IgG (H+L, code: 715-035-150) were provided from Jackson ImmunoResearch Laboratories, inc.

3.9 SDS-polyacrylamide gels

The following reagents were used for the SDS - polyacrylamide gel electrophoresis (SDS-PAGE) gels to yield an acrylamide concentration of about 10%. For one running gel a total volume of 5.0125 mL was made containing 1.67 mL 30% Acrylamide/Bis Solution (Bio-Rad Laboratories Inc, China), 2.83 mL ddH_2O, 0.5 mL 10X TGS 10 µL 10% ammonium persulfate (Bio-Rad, catalog number 161-0700) and 2.5 µL TEMED (BIO-RAD laboratories Inc, US). One stacking gel was prepared with 1.53 mL ddH_2O, 325 µL 30% acrylamide, 625 µL 0.5M Tris-HCL pH 6.8, 25 µL 10% SDS, 12.5 µL APS and 2.5 µL TEMED.

3.10 Western blotting

All buffers mentioned below were prepared for western blotting and were commercially supplied by Bio-Rad Laboratories GmbH or Sigma-Aldrich if not else annotated. Sodium dodecyl sulphate (SDS) polyacrylamide gels were prepared in-house to an approximate concentration of 10% acrylamide (see section for SDS-polyacrylamide above). Cellular lysates of 40 µg or 30 µg per sample were diluted in Loading buffer (final concentration of 1% SDS, 10% Glycerol, 12 mM Tris-HCl pH 6.8, 50 mM DTT, and 0.1% Bromophenol Blue [v/v]) to a total volume of 30 µL. Samples were denatured at approximately 99 ºC for 5 minutes, placed on ice to cool down samples and spun down briefly prior to loading onto the gels alongside a pre-stained standard (Precision Plus Protein ™ Standards All Blue, Bio-Rad Laboratories, Catalog # 161-0373, Hercules, Ca, USA), permitting protein molecular weight estimation.

Proteins were separated by size by SDS-PAGE using SDS-polyacrylamide gels and 1xTGS running buffer (10xTris/Glycine/SDS (TGS) containing 25 mM Tris-base, 192 mM Glycine, 0.1% (w/v) SDS, pH 8.3 diluted in dH_2O) at 150 V for approximate 1 hour. Electroblotting was performed using Polyvinylidene fluoride (PVDF) membrane (Bio-Rad Laboratories, Inc. US) and transfer buffer (10% methanol, (Sigma-Aldrich), 80% dH_2O, 10% 10xTris/Glycine Buffer[TG, 25 mM Tris, 192 mM Glycine, pH of 8.2]) over night (4 ºC) or at room temperature (RT) for 90 minutes, 100 V. After blocking for prevention of nonspecific protein binding for 1 hour with 1x TBS, 1% Tween®20 (SIGMA-Aldrich, France) (TBST) and 5% Bovine Serum Albumin FractionV (BSA) (Roche, GmbH Mannheim, Germany), the membranes were rinsed three times ten minutes with washing buffer, 1X TBST. Thereafter the membranes were incubated with primary antibodies (1:1000) to pERK, p21, caspase 8, HK1, HK2, diluted in 1X TBS, 1% Tween®20, 5% BSA overnight at 4ºC. Gapdh and cox IV served as internal loading control for equal loading of protein content. They serve as loading controls as they are constitutively expressed in all cells and suggested not to be affected by the drugs which have been explored in this thesis. Membranes were washed as described above to remove unbound primary antibody, prior to incubation with horseradish peroxidase (HRP)-conjugated rabbit antirabbit or antimouse antibodies (1:1000, Jackson ImmunoReasearch Laboratories, West Grove, PA, USA), diluted in washing buffer containing 5% BSA, for 1 hour at RT. The membranes were then rinsed thrice in washing buffer prior to detection. Antibody detection of the target protein was accomplished by exposing the protein bound HRP labeled antibody to a solution of chemoluminiscent substrates

(chemoluminescence detection kit: SuperSignal®West Pico/Femto Stable peroxide solution, Thermo Scientific, U.S. [1:1]). Protein bands were visualized by light emission captured by the Luminescent Image analyzer (ImageQuant LAS 4000, GE Healthcare, Denmark). A relative comparison of protein level was quantified using the ImageQuant TL Analysis program. In short, the background noise was subtracted prior to detection of bands by the software. The volume of material in the band at the detected position (R_f = relative migration distance) was quantitated. The data were then exported to Excel spreadsheet and fold change was calculated by dividing the value from the volume of protein of interest by the value of volume of loading control. The value obtained was then normalized to the loading control (gapdh, coxIV).

3.11 siRNA

HL60 cells were cultured as previously described. The siRNA duplexes were designed to target the regions of HPRT1 mRNA and HK1 mRNA and were synthesized by Qiagen Research, Inc. Hilden, Germany. The transfection of siRNA was performed by following the suppliers' instruction (Invitrogen) using the Neon™ device with Neon™ Pipette Station and Neon™ Kits (Invitrogen, Carlsbad, CA, USA). The electroporation parameter for HL60 was previously optimized to 1325V, width 35 ms with 1puls per electroporation. MOLM13 cells were exposed to one puls of 20 ms with 1725 Volt, whilst NB4 cells had 3 pulses with width of 10 ms at 1700 Volt. 10 µl of 20 × 10^6 cells/ml (Resuspension buffer [RB]) were electroporated with HK1(FlexiTube, Cat. No. SI00004193, QUIAGEN), HPRT1 siRNA (FlexiTube, Cat. No. SI00004193) or negative control (AllStars Negative Control Alexa Fluor 488 siRNA, Qiagen) (final concentration 600 nM) using the disposable Neon tips as electroporation chamber. Cells were transferred to a 96 well plate containing pre-warmed RPMI—1640 medium supplemented with 10% FBS and 1% LG without antibiotics, 50 µM LND, 0.1 µM MMF or 1 mM VPA was added after 18 hours incubation siRNA only, before cells were incubated for an additional 48 hours. WST-1 proliferation assay was used for the analysis of metabolically active cells, prior to scoring of abnormal nuclei as described above. To evaluate the proliferation effect of the electroporation process itself, untransfected cells were compared to cells electroporated without siRNA. The AllStars Negative Control AlexaFlour488 siRNA has no homology to any known mammalian gene and was therefore used as negative control for siRNA effect, as well as control for siRNA transfection efficiency. Furthermore, three different mock transfection controls consisted of cells in RB,

whereof two contained either of the drugs used in the experiments. Data were normalized as following prior introducing to GraphPad Prism; electroporated samples without knockdown were normalized to electroporated sample treated with vehicle only (DMSO), whilst siRNA of interest (HPRT1, HK1) introduced samples were normalized to negative siRNA control (AF488).

3.12 Statistical Analysis

Throughout the thesis, the graphical representations of the *in vitro* and *in vivo* data were given as the mean ± standard deviation (SD).

The evaluation of drug combination efficacy was based on the Bliss Independence model. The actual combination response was compared with the response to be expected. The expected response value was obtained by using the following formula:

$$Y_{ab} = Y_a + Y_b - (Y_a Y_b),$$

where a resemble the fraction of positive effect by drug A, and b the fraction of the positive effect of drug B. If the actual response was higher than the expected (Y_{ab}) effect of the two drugs, the combination was considered to have a synergistic effect.

The IC_{50} was obtained by using the IC50 Downloaded Prism file from the software GraphPad Prism 6.0. A nonlinear regression fitted the normalized data to a dose-response curve of log-transformed concentrations (inhibitor) vs. response (variable slope) curve. The relative IC_{50} was calculated by the antilog of the value obtained by the software. Negative control constrains the top plateau (dotted) lines to 100% in experiments resulting in an enhanced effect of metabolic cell activity following drug treatment for an optimal IC_{50}.

Statistical correlation coefficient (r) was calculated by using the CORREL Stats function in Excel spreadsheet based on the Pearson`s Correlation. This statistical value was used for determining how well associated two variables are. The variables in this thesis were normalized percentages of metabolically active cells (WST-1) or viable cells (Hoechst staining, Annexin-V/PI). The Pearson`s Correlation formula uses the notations:

$$r = \frac{n(\sum xy) - (\sum x)(\sum y)}{\sqrt{[n\sum x^2 - (\sum x)^2][n\sum y^2 - (\sum y)^2]}}$$

Where x are the sample variables from for example Hoechst viability assay, whilst y represent those obtained from Annexin-V/PI.

All statistical interaction testing were made with a Two-way ANOVA test complemented with Turkey`s multiple comparison test, whilst comparisons of two variables with minimum sample size of 3 were performed using standard two-sided Student`s t-test.

4. Results

4.1 Assessing the Anti-leukemic Effect of Mycophenolate mofetil in Combination with Valproic acid

The survival benefit of the HDACi VPA is only observed for a minority of AML patients (20-30%). Alternative co-therapeutics has previously been explored by VPA treatment in the *in vivo* BNML-rat model in order to improve the responsiveness among subgroups of AML patients. (3) Here they found a reduced expression of phosphorylated HPRT1. This enzyme of the purine nucleotide synthesis may be an alternative target sensitized by MMF.
Selected human AML cell line models representing AML with limited differentiation (HL60, MOLM13, NB4; FAB M2, M4/5) and promyelocytic leukemia (NB4; FAB M3) displaying comparable genetic profile to a subset of AML patients, were treated with a concentration range of MMF (0.025-2.5 µM) for 48 hours, based on previous drug screen. (96) In order to assess the suitability of MMF as an anti-leukemic agent, distinct preliminary drug screening assays investigating apoptosis and proliferation were performed on cells following drug exposure.

4.1.1 The metabolism inhibiting effect of MMF

The metabolism assessed with WST-1 assay evaluated the rate of proliferation (methodology; section 3.4). **Figure 2 A-C** illustrates the sensitivity of the different cell lines to MMF following 48 hours of treatment. The results suggest that MMF possesses a capacity of a dose-dependent suppression in that the metabolism is turned down, but the number of cells is the same.

Drug efficacy varies among patients, which was correspondingly observed in **Figure 2 A-C** for the cell lines treated with MMF. The IC_{50} (inhibitory concentration) (**Figure 2 D-F)** predicts the sensitivity of the AML cells lines to MMF. The IC_{50}s ranging from 0.048 to 0.307 µM indicates that MMF is more effective in MOLM13 (0.048 µM) and NB4 (0.103 µM) compared to HL60 cells (0.307 µM). Nonetheless, due to higher standard deviations in HL60 and MOLM13 (not obtainable by GraphPad), the IC_{50} values for MMF in both cell lines may be present in wider range of concentrations presented as the 95% Confidence Interval (CI). Vertical dotted lines in **Figure 2 D-F** define the inhibition interval of MMF, whereof the

bottom line represents maximal inhibition of the drug in the particular cell line. The percentage of metabolic activity decreases more rapid in NB4 and MOLM13 cells versus HL60 when reaching half maximal inhibitory concentration of the slope (**Figure 2F**), but the efficacy of the drug for all three cell lines was to some extent similar when treated with 0.5 µM and 1 µM MMF and varied more between the cell lines at concentrations lower than 0.5µM MMF.

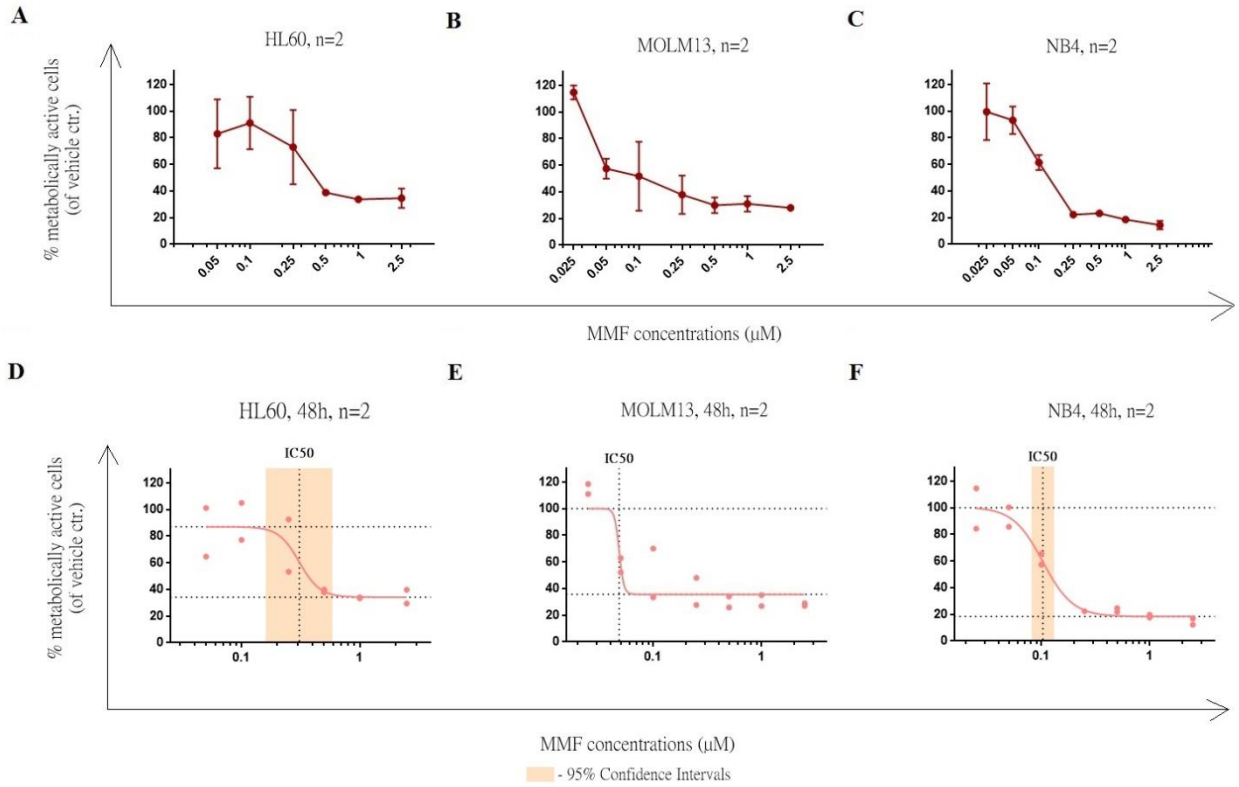

Figure 2. Reduced metabolism by MMF in AML cell lines. Oxidoreductase activity was measured after MMF treatment for 48 hours by WST-1 conversion in HL60 cells **(A)** MOLM13 cells **(B)** and NB4 cells **(C)**. Results were normalized to negative control containing cells in culture with vehicle (DMSO) only, and are presented as the mean ± SD of two independent experiments. IC_{50} (vertical dotted line) was calculated in HL60 (0.307 µM, CI: 0.160 – 0.589 µM) **(D)**, MOLM13 (0.048 µM, CI: not obtainable) **(E)**, and NB4 cells (0.103 µM, CI: 0.080 – 0.130 µM) **(F)** as described in section 3.12. Vertical dotted lines define the inhibition interval of MMF, whereof the bottom line represents maximal inhibition of the drug for each cell line. IC_{50}s interval for MOLM13 was constrained by the control due to an increased activity of metabolic cells. Pink shaded area in graphs displays 95% Confidence Interval (CI) of MMF.

4.1.2 MMF induces apoptosis in AML cell lines

The percentage of viable cells with normal nuclear morphology was attained by counting normal versus abnormal nuclei (nuclear fragmentation, condensation) (**Figure 3B**) labeled with the double-stranded DNA staining fluorescent dye Hoechst 33342. The evaluation of

cells with normal nuclear morphology showed that all three cell lines responded comparably similar to all concentrations with MMF, except from the two highest concentrations (1.0 µM and 2.5 µM) resulting in higher extent of apoptotic cells in NB4 in comparison to HL60 and MOLM13. A clear difference was observed in the amount of viable cells in all three cell lines when treated with low dose (0.05 µM) versus high dose (1.0 µM) MMF.

A

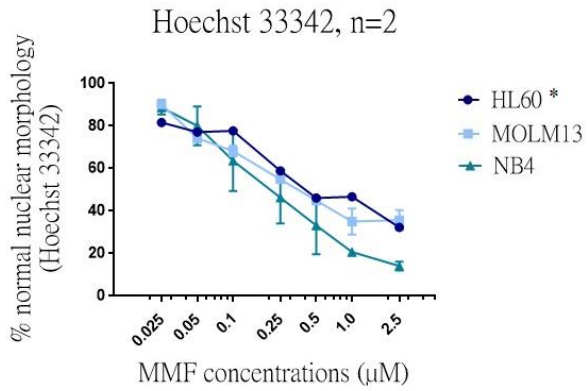

B

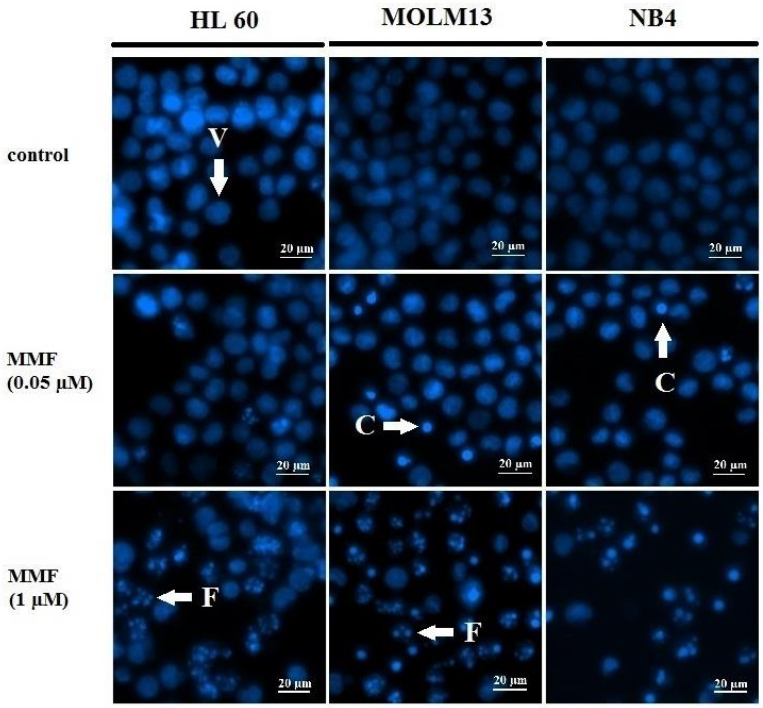

Figure 3. Cell viability by DNA fluorescence staining following treatment with MMF (A) Percentage of cells with normal nuclear morphology normalized to negative control containing cells added vehicle (0.025 % DMSO). Two independent studies (*n=1) is presented. The reduction of normal cell morphology in HL60 cells is illustrated in dark blue, MOLM13 in light blue and NB4 in turquoise. **(B)** Fluorescence microscopy visualizing Hoechst 33342 stained dsDNA of HL60, MOLM13, and NB4 cells treated with either the low dose 0.05 µM or high dose 1 µM MMF. Scale bar (20 µM) shows the degree of magnification of the image. C – Condensed apoptotic nuclei, F – fragmented apoptotic nuclei, V – viable cell nuclei.

4.1.3 The effect of MMF on proliferation of PBMCs and AML patient blasts

To investigate the potential adverse toxic effect of MMF to the peripheral immune system function, normal peripheral blood mononuclear (PBMC) cells were treated with MMF. Results from WST-1 assay showed no decrease in metabolic activity (**Figure 4**, circles) suggesting that the proliferation of normal PBMCs is not affected by MMF when incubated for 48 hours with a range of concentrations (0.25 – 2.5 µM). To explore the *in vitro* effect of MMF in AML patient cell, blasts from two patients were treated with MMF under the same conditions as the PBMCs (**Figure 4**, squares and triangles). The metabolic activity of blasts from patient 1 is not reduced when treated with MMF for 48 hours, whereas blasts from patient 2 are more sensitive to MMF at lower doses (0.1 – 1.0 µM). The *de novo* AML Patient 1had a complex karyotype (≥ 3 acquired chromosome aberrations) with wild type FLT3 and wild type NPM1. Comparably, HL60 cells also have an intact FLT3 and showed less responsiveness to MMF **(Figure 2A)**. Patient 2 AML cells had normal cytogenetics (karyotype 46 XY). FLT3 tyrosine kinase domain mutation ratio was shown to be low (0.07) with an internal tandem duplication (ITD) in exons 14 and 15. The presence of ITD confers an increased risk of relapse and death. (128) A typical 4-bp insertion mutation clustered within exon 11 was detected in the NPM1.

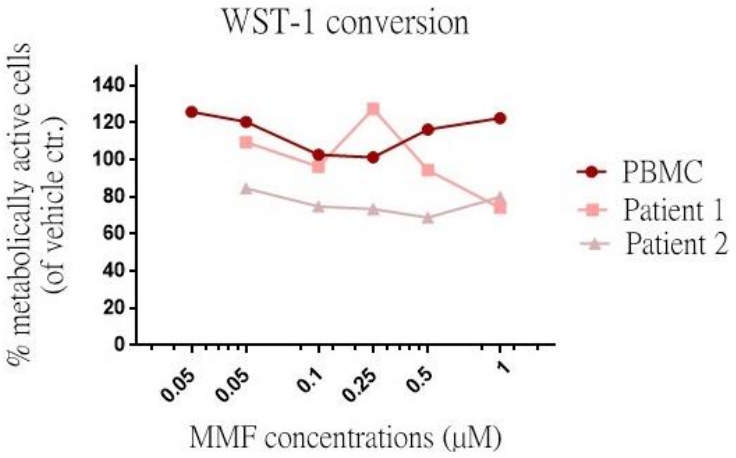

Figure 4. Cell proliferation in primary AML patient blasts and PBMCs treated with MMF for 48 hours. PBMCs were studied in one healthy donor for a wide range of MMF concentrations (0.025 – 2.5 µM) whilst both AML patient derived samples were treated with five distinct MMF concentrations (0.1 – 2.5 µM).

4.1.4 No potential benefit from the combination treatment of MMF and VPA

This section demonstrates the results with particular interest on whether MMF, an inhibitor of the adenosine and guanosine nucleotide biosynthesis, work in tandem with the HDAC Class I and II inhibitor VPA and if it represents a useful manner of enhancing the efficacy of VPA and MMF alone as anti-leukemic agents. (5, 60) The drug screening in the previous sections suggests that all three cell lines respond to the pro-apoptotic and anti-proliferative effects of MMF **(Figure 2 and 3)** alone. **Figure 5** demonstrates that VPA by itself elicits minor anti-leukemic effect at concentrations lower than 0.5 mM with various sensitivities to all three cell lines. NB4 were more sensitive to VPA at concentrations from 0.5 mM to 2.5 mM when analyzed by WST-1 based proliferation- and Annexin-V/PI viability assays **(Figure 5A, C)**. The quantity of metabolically active NB4 cells was reduced by 38% after 48 hour exposure to 0.5 mM VPA, whilst 58% of the treated cells were considered viable. MOLM13 responded to 0.5 mM VPA by a decrease in 36% metabolically active cells and 93% viable cells, whereas HL60 showed a lower degree of sensitivity to concentrations higher than 0.25 mM VPA in both viability and proliferation compared to NB4 and MOLM13. **Figure 5** Illustrates the capacity of MMF (0.1-2.5 µM) and VPA (0.1-2.5 mM), used alone and in combination to reduce the quantity of metabolically active cells and to decrease the viability by inducing apoptosis in HL60, MOLM13 and NB4 human AML cells. MMF and VPA cooperated in less than additive manner to both reduce the percentage of metabolically active cells **(Figure 5A)** and to decrease the presence of viable cells **(Figure 5B, C)**. Flow cytometric analysis confirmed data obtained from microscopy evaluation of apoptosis (**Figure 5B**). Acquired data from Annexin-V/PI apoptosis detection assay showed larger viable population of MOLM13 cells obtained by co-treatment of VPA (0.25 mM – 1 mM) and MMF (0.25 µM – 1 µM) in contrast to when cells were treated with one drug only **(Figure 5C)**. This was also observed for NB4 cells at the two highest combination treatment concentrations (1 µM, 2.5 µM MMF, 1 mM, 2.5 mM VPA). The ability of co-treatment-provoked apoptosis in HL60 cells was analyzed by Hoechst 33342 viability assay **(Figure 5B)**, showing no substantial decrease in viable cells compared to what is obtained by MMF single drug treatment **(Figure 5A)**. There was no significance in the combined effect of MMF and VPA in all three cell lines evaluated both proliferation and apoptosis (Hoechst 33342) when tested for Two-way ANOVA Turkey`s multiple comparison test and Bliss Independence model (section 3.12) did not indicate synergism for the combined treatments with MMF and VPA in all three cell lines evaluated by both proliferation and apoptosis (Hoechst 33342). The absence of synergism is

exemplified using MOLM13 cells (0.5 µM MMF, 0.5 mM VPA) in **Figure 6** where the expected amount of metabolically active and viable cells behind was not accomplished.

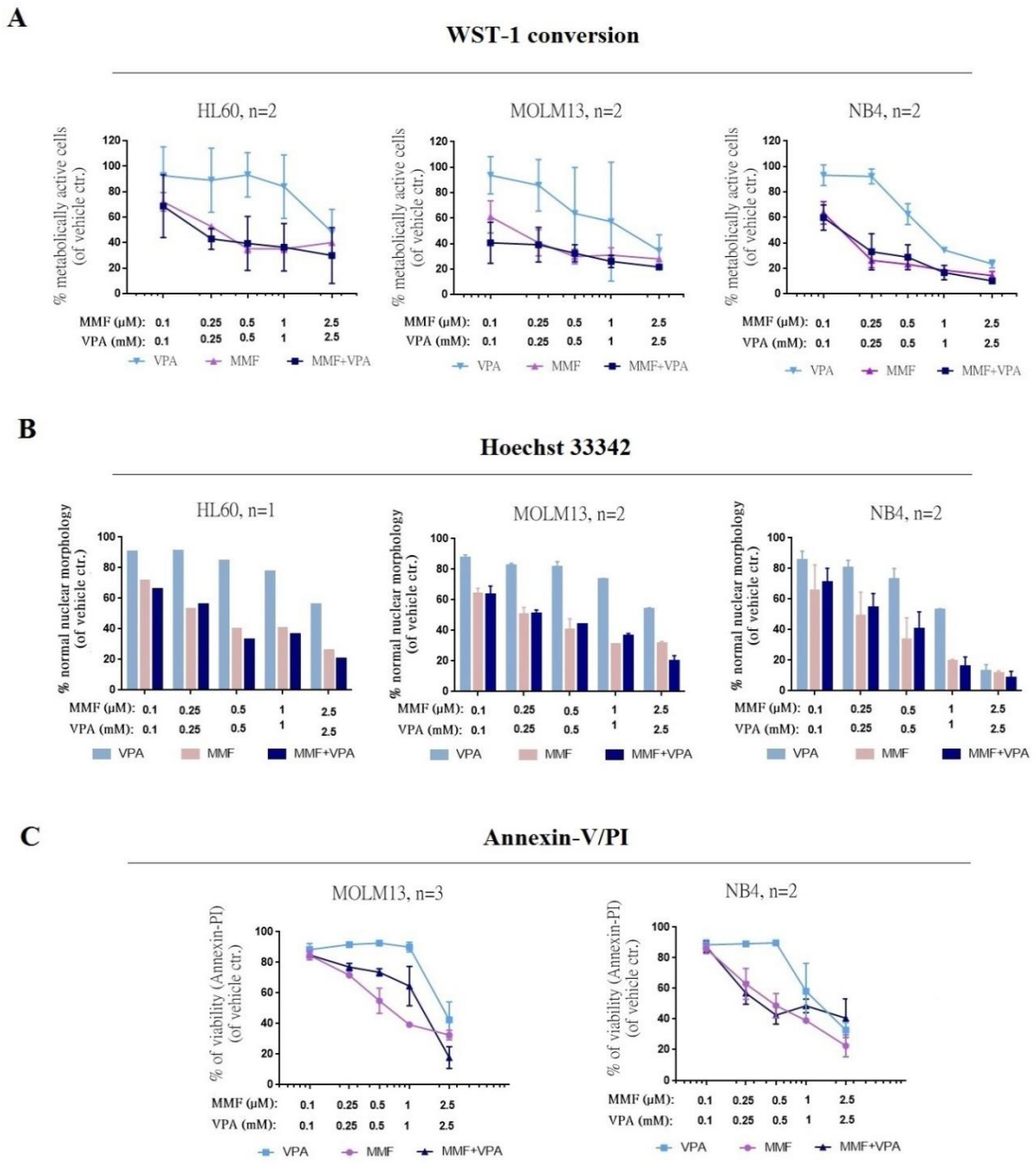

Figure 5. Effect of single-drug treatment and combination treatment of MMF and VPA on proliferation and viability of human AML cell lines. (A) Metabolically active cells in HL60, MOLM13, and NB4 cells obtained by WST-1 proliferation based assay following 48 hour treatment of MMF, VPA, and in combination with concentrations in fixed ratio. Results are given as mean ± SD from two independent studies for each cell line. **(B)** Cell viability detected by Hoechst 33342 and analyzed in a single study for HL60, MOLM13 and NB4 cells. **(C)** Annexin-V/PI flow cytometry analysis confirmed the sensitivity for MMF, VPA and combination treatment. The percentage of viability of control in three (MOLM13)/ two (NB4) independent studies is presented with mean ± SD from MOLM13 and NB4 cells. 5000 events were measured for each concentration.

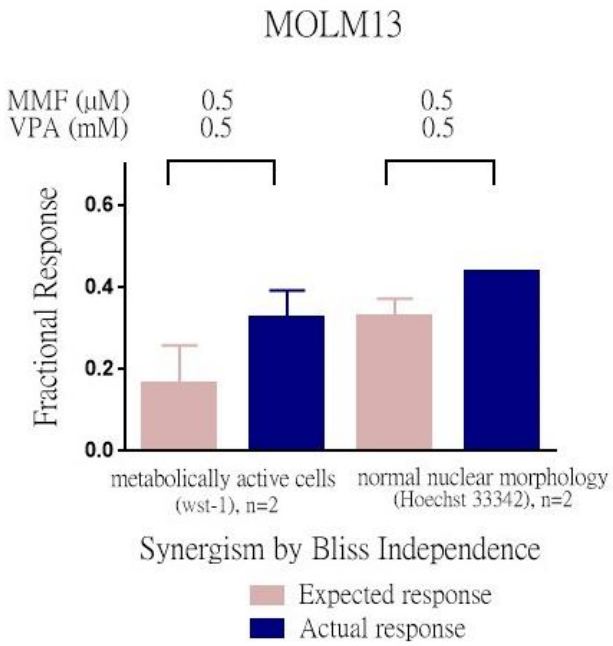

Figure 6. Testing for synergism with Bliss Independence Model for the effect of the combinational treatment of MMF (0.5 µM) and VPA (0.5 mM) on MOLM13 cells. Graph exemplifies the absence of synergism which was calculated for all three cells lines (not shown). Expected fractional response of metabolically active cells versus actual response of co-treatment is presented with means ± SD of two independent studies, obtained from WST-1 proliferation based assay. Expected versus actual response of apoptosis induction was analyzed by Hoechst 33342 by the discrimination of normal and abnormal nuclear morphology.

4.1.5 The Investigation of MMF in Additional Drug Combinations

All three human AML cell lines in this project showed responsiveness to MMF. Nonetheless, MMF did not enhance the anti-leukemic effect of VPA that in particular was the main interest with the use of MMF. However, the preliminary results obtained with MMF lead to the interest to investigate its attribute in a cooperative manner with other agents. The combined treatment of MMF with the well-established agent Hydroxyurea (HU) was further investigated. Interestingly, both drugs interfere with the nucleotide synthesis. MMF interferes with the conversions from precursors to GMP and AMP, while HU affects up-streams of MMF by the conversion of ribonucleotides to deoxyribonucleotides. (56) The combined effect of HU and MMF, shown in **Figure 7A**, followed the same anti-proliferative response to that of MMF alone and no additive effect or synergism was achieved. As both HK1 and HPRT1 were down-regulated by VPA in BNML rats, the combination of LND and MMF **(Figure 7B)** was investigated for potential synergistic or additive effect on proliferation and apoptosis. (3)

This combination neither showed significant enhanced potentiation of MMF nor LND.

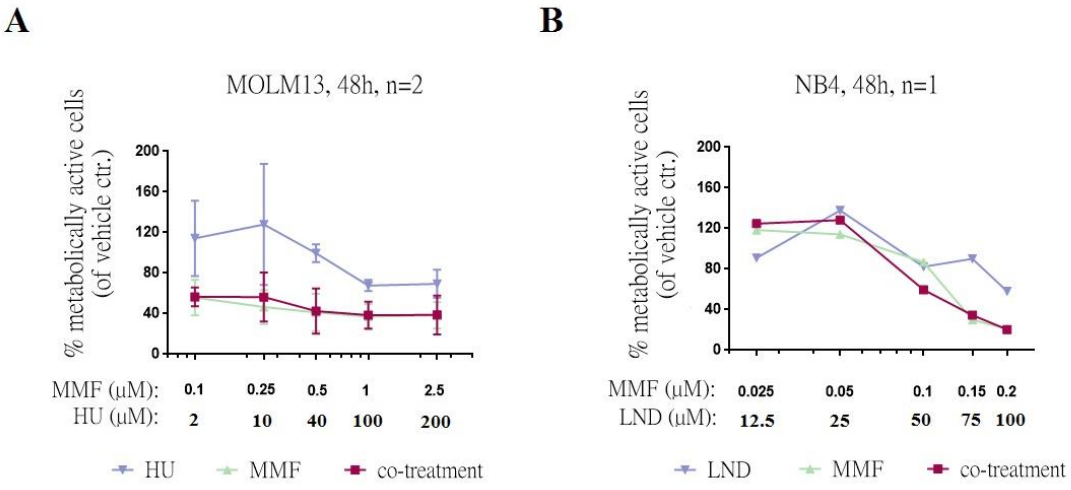

Figure 7. Combination treatments exploring the potential utility of MMF as a cooperative drug with other agents. WST-1 proliferation based assay was applied for the pilot experiments; **(A)** MMF with literature based concentrations of HU (129), in two independent treatment studies of MOLM13 cells for 48 hours, and **(B)** one study of MMF combined with LND in NB4 cells (48 h).

4.1.6 Transient suppression with unmodified HPRT1 siRNA changed the effect by VPA treated HL60 cells

Promising synergistic effects were not obtained *in vitro* from the combination treatment of MMF and VPA on HL60, MOM13 and NB4 cells. Thus, knockdown of HPRT1 was performed to elucidate whether a more specific direct targeting of the enzyme can increase the anti-leukemic effect of VPA. HL60 was found to be the least sensitive cell line to MMF at lower concentrations, where 0.1 µM resulted in approximately 70% metabolically active cells. In order to investigate the influence of MMF on HPRT1-signaling in HL60 cells, HPRT1 siRNA was directly introduced into HL60 cells by electroporation using Neon Transfection system allowing knockdown of HPRT1. For the establishment of a balance between cell viability after transfection and delivery efficiency, optimized variables for each electroporation of HL60 cells were previously determined. The change in proliferation by HPRT1 knockdown was examined by WST-1 conversion **(Figure 8)**. The electroporation procedure was observed to be tolerated by the cells affecting the reduction of only 3% metabolically active cells. Scrambled negative siRNA control to AF 488 dye, demonstrated the transfection efficiency. Quantification of successfully transfected cells was not obtained from this study. **Figure 8** shows no difference of the extent of metabolically active cells between HPRT1 siRNA transfected and un-transfected cells, treated with vehicle only. This

suggest that knockdown of HPRT1 does not result in decreased level of metabolically active cells by itself. Treatment with MMF on cells with HPRT1 knockdown did not lead to a change in the effect on proliferation from what is obtained with MMF alone. These data demonstrate that no further enhanced effect from MMF to reduce proliferation in HL60 cells was achieved by knockdown of HPRT1. However, knockdown of HPRT1 in HL60 cells measured 48 hours after addition of VPA affected the rate of metabolically active cells. This enhanced treatment effect in HL60 cells, compared to from what is obtained by VPA alone, suggests for an increased anti-leukemic effect with VPA when combined with a HPRT1 specific targeting agent. But for the findings of this experiment to be of statistical significance and not due to chance, further replicates are needed.

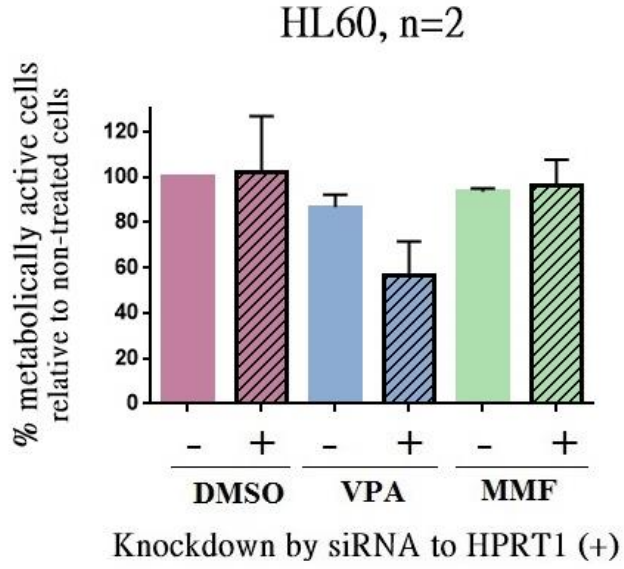

Figure 8. Effect of gene specific knockdown by HPRT1 siRNA in HL60 cells. siRNA (negative control AF488 and HPRT1) was introduced to cells by electroporation prior to incubation for 18 hours and subsequent treatment with MMF (0.1 µM) or VPA (1 mM) for additional 48 hours in two technical replicates of one experiment. The metabolism inhibiting effect on cells was assessed by the WST-1 proliferation assay. HPRT1 knockdown caused no change in effect of MMF on proliferation, whilst the potential of VPA to reduce proliferation was improved. Electroporated samples with no transfection (-) were normalized to electroporated sample treated with vehicle only (DMSO), whilst siRNA (HPRT1) introduced (+) samples were normalized to negative siRNA control (AF488). Means ± SD are displayed by error bars.

4.2 Effect of Lonidamine in HL60, MOLM13 and NB4 cell lines in *in vitro* experiments

Lonidamine (LND) has been reported to elicit poor cytotoxic effect by itself but to augment the efficacy of other antineoplastic drugs. (106, 111) Only at concentrations higher than 100 µM, LND has shown to reduce the viability of cancer cells. The following sections present

results that can support the reproducibility of experiments with LND holding properties such as anti-tumorigenecity.

4.2.1 Assessing appropriate LND exposure time by Proliferation Assay and IC_{50}

All three AML cell lines (HL60, MOLM13, NB4) were exposed to increasing concentrations of LND (1 – 500 µM) for 24 and 48 hours in a dose range previously described by others in various cancer cells, mainly solid tumors. (130) The comparative sensitivity of each cell line to LND for 24 hours is presented in **Figure 9A**. No significant difference ($P > 0.05$) in reduced metabolically active cells was obtained between HL60 and NB4 cells after 24 hour treatment with LND. Both cell lines responded by approximately 20% reduced metabolically active cells at concentrations lower than 50 µM LND. Higher concentrations (> 100 µM) of LND were needed for a significant ($P = 0.0105$) decrease in metabolically active MOLM13 cells. There was no strong evidence that HL60, MOLM13 and NB4 cells responded different to treatment with higher concentrations of LND (> 50 µM). IC_{50}s of LND was obtained from WST-1 proliferation assay, and are presented in **Figure 9B**, **C** and **D** for HL60 (149 µM), MOLM13 (218 µM) and NB4 (203 µM), respectively. A wider 95% CI is observed for the IC_{50} of LND in treated NB4 cells (**Figure 9D**) than for HL60 and MOLM13, thus we cannot exclude the possibility that the IC_{50} of NB4 could be present anywhere between 106 – 387 µM. The inadequate PBMC sample size limited statistical evaluation of the difference in effect by LND on proliferation in PBMC versus AML cell lines. Nonetheless, **Figure 9A** illustrates that the sensitivity of MOLM13 to LND is not higher than to what is observed for the PBMCs when treated for 24 hours.

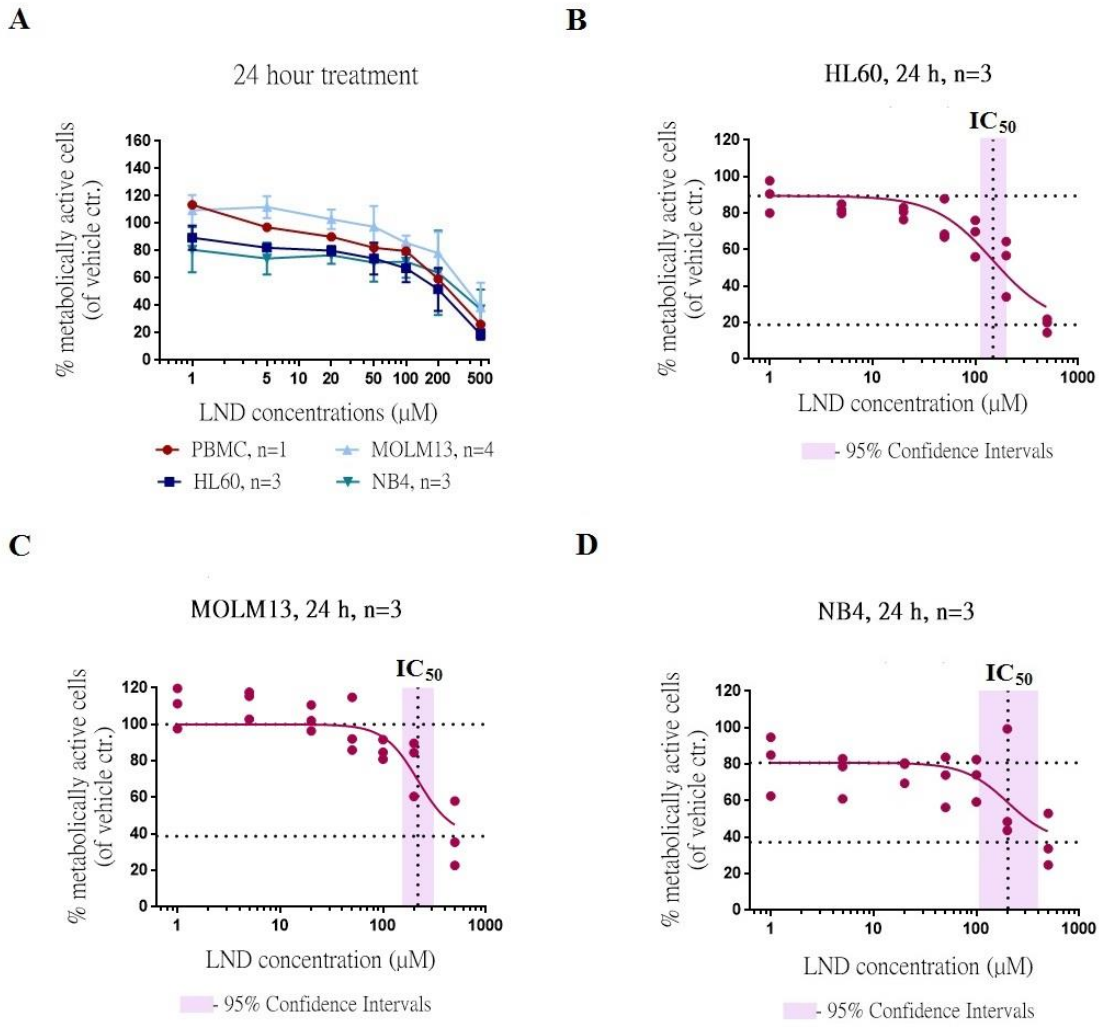

Figure 9. Minor decrease in metabolically active cells following 24 hours treatment with LND. (A) HL60, MOLM13, NB4, and PBMC response on metabolic activity following LND exposure**. (B)** HL60 (149 µM, CI: 110-200 µM), **(C)** MOLM13 (218 µM, CI: 153 – 311 µM), and **(D)** NB4 (203 µM, CI: 106 – 387 µM) dose response curves displaying IC_{50} values (vertical dotted line) between the maximal response (top horizontal dotted line) and the maximal inhibited (bottom horizontal dotted line) response of the drug. Purple shaded area displays 95% CI of IC_{50} value.

The efficacy of LND to reduce proliferation in HL60 was similar to when exposed for 24 hours, whilst NB4 cells responded by an increase in proliferation at concentrations lower than 100 µM. Increased LND incubation time from 24 hours to 48 hours significantly ($P < 0.05$, 20 µM – 500 µM LND) ($P < 0.0034$, 5 µM LND) affected proliferation of MOLM13 cells. The distinct response of PBMC comparable to MOLM13 and HL60 is noticeably demonstrated in **Figure 10A.** NB4 was significantly ($P < 0.05$) more sensitive to LND under 24 hours of exposure than 48 hours (5 – 500 µM). The IC_{50} of LND in NB4 (201 µM), HL60 (248 µM) and MOLM13 (124 µM) are presented in **Figure 10 B, C** and **D** indicating LND to be more effective after 48 hour treatment in MOLM13 and NB4 cells at lower concentrations

than when treated for 24 hours. The 95% CI for NB4 was very wide and not obtainable by GraphPad Prism due to an increase in percentage of metabolically active cells.

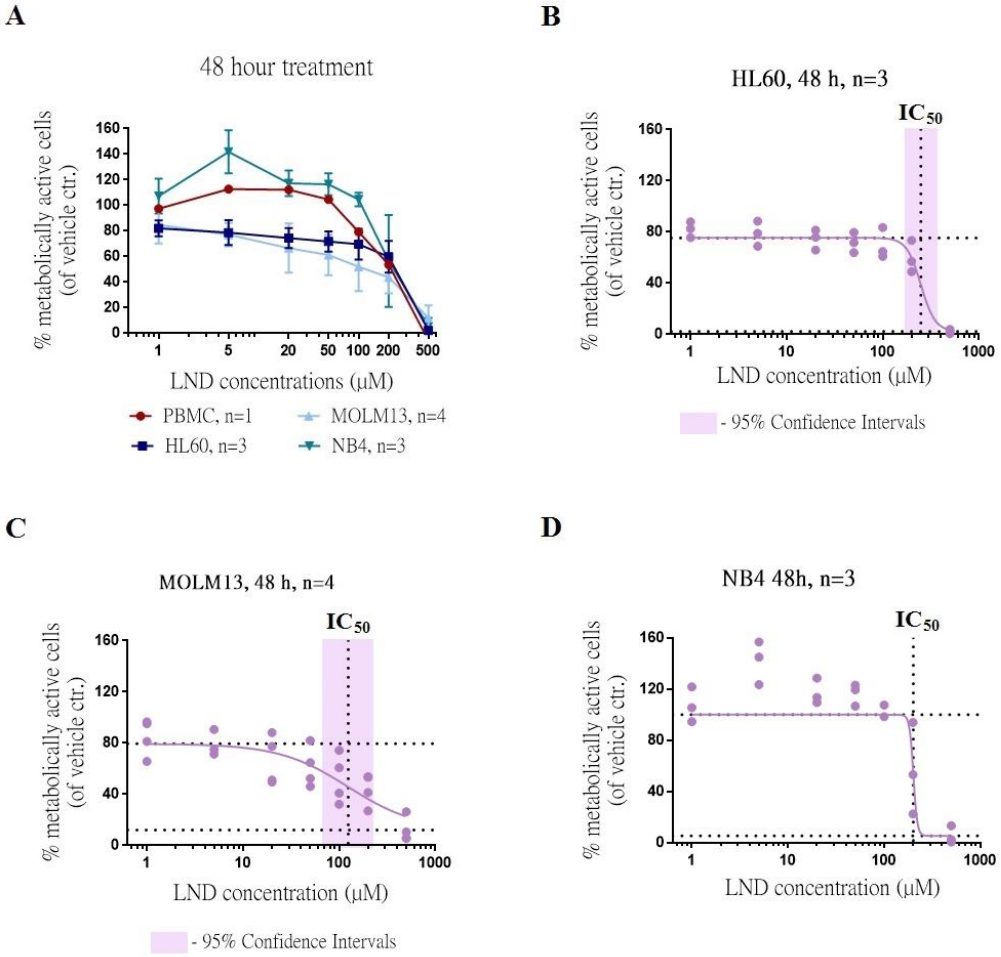

Figure 10. Reduced cellular oxidoreductase activity following 48 hours treatment with LND. (A) PBMC and NB4 cells increased in metabolically active cells at concentrations < 50 µM and 100 µM, respectively, whilst MOLM13 and HL60 enhanced sensitivity to LND compared to 24 hour exposure. Half maximal inhibitory response (vertical dotted line) was assessed from WST-1 conversion data in **(B)** HL60 (135 µM), **(C)** MOLM13 (46 µM) and **(D)** NB4 (182 µM) cells. 95% CI is presented in purple shaded area in graph. (NB4 CI was not obtainable)

4.2.2 Apoptosis induction by Lonidamine of human AML cell lines

LND elicits potential of inducing apoptosis after both 24 hours and 48 hour incubation at higher concentrations (> 50 µM) in HL60, MOLM13 and NB4 **(Figure 11A-B).** Apoptotic cells in the stage of morphological changes such as fragmented or condensed nuclei are shown in **Figure 11C**, visualized by fluorescence microscopy. The frequencies of abnormal nucleic morphology were minor at concentrations lower than 50 µM in all three cell lines. However, the incidence of cells being in an earlier apoptotic stages may be present but not

detected under examination. Cells may therefore be likely in a pre-apoptotic phase induced by lower concentrations of LND.

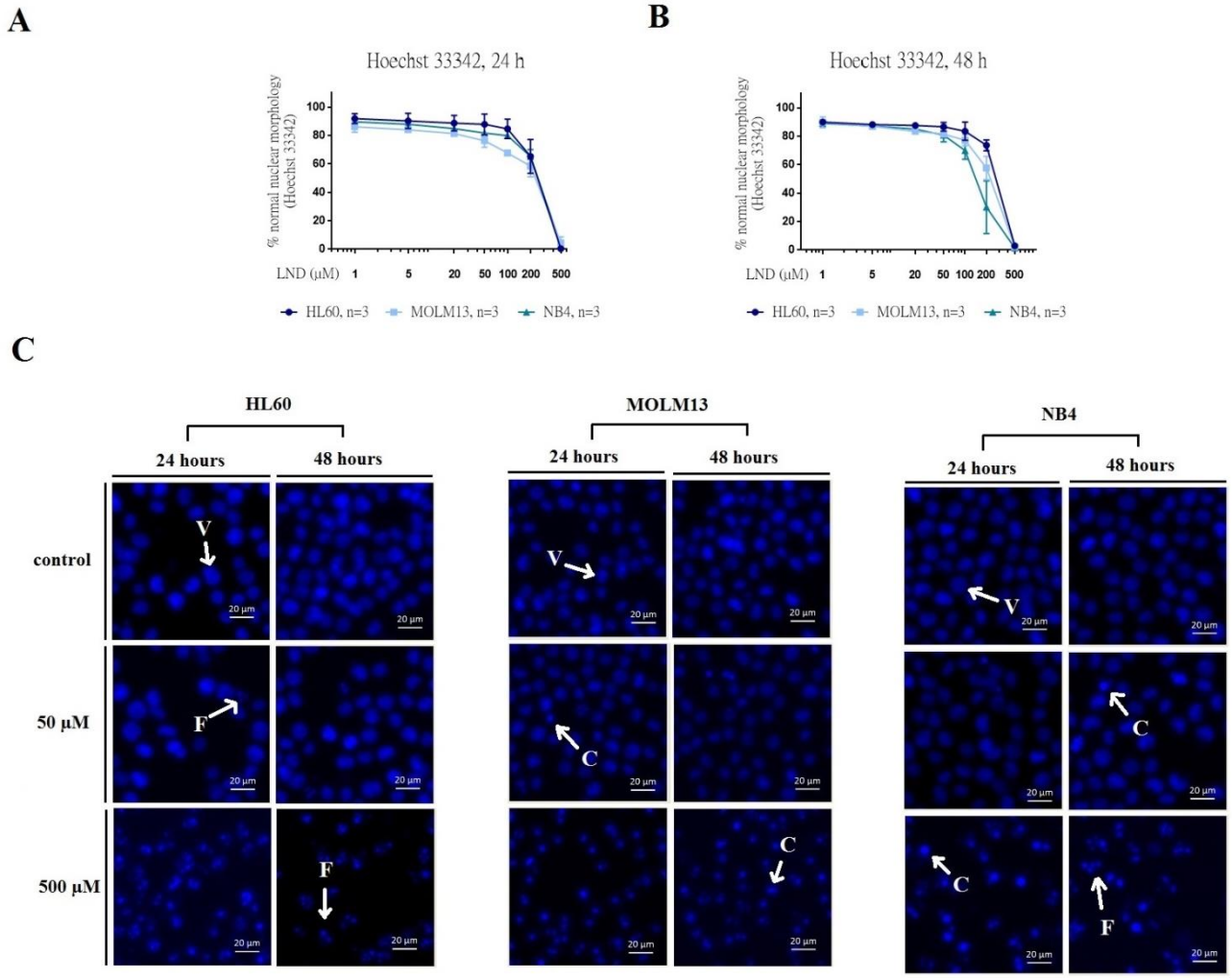

Figure 11. Effect of LND on cell viability in human AML cell lines following exposure of 24 and 48 hours. Quantification of abnormal nuclei after three independent treatment-studies of LND in HL60, MOLM13 and NB5 cells for **(A)** 24 hours and **(B)** 48 hours. Error bars are presented as means ± SD. **(C)** Nuclei presented in both apoptotic and viable morphology, visualized by Hoechst 33342 staining and scored as: V – Viable cells, C – condensed apoptotic nuclei morphology, F – fragmented apoptotic nuclei. Scale bar: 20 µM.

4.2.3 Dose Dependent Synergistic Effect of Lonidamine and Valproic Acid

Few studies have investigated the potentiation of LND activity to enhance drug cytotoxicity in a dose and schedule dependent manner. (131) Thus sequence administration **(Figure 12)** and optimization of treatment with LND (50 and 100 µM) in combination with VPA (0.5 and 1 mM) was performed. These are concentrations that showed enhanced potential of anti-proliferative activity when combined **(Figure 13A)** in the least sensitive cell line HL60,

examined in this project**.** The concentration of VPA that, by itself, reduced the surviving fraction of target AML cells by approximately 10 % (0.5 mM and 1 mM) was chosen. HL60 cells were exposed to the drugs in two different sequences; LND incubation for 24 hours prior to 48 hours combined treatment with VPA and LND (LND → VPA+LND) and the reverse (VPA → LND+VPA). This sequenced treatment was compared to a 48 hour combined study, without pre-treatment of LND or VPA, to investigate whether LND could enhance the anti-proliferative effect of VPA against the human AML cell line HL60. The results were normalized to the negative control with vehicle only (DMSO [v/v%]) and plotted as a logarithmic graph **(Figure 12).** Maximal potentiation of LND was obtained by 100 µM LND in the sequence VPA → LND+VPA, but no significant increased anti-proliferative effect was obtained from three independent and replicable studies. These preliminary results are supported by previous experiments showing the anti-proliferative effects of VPA to increase with increasing exposure time. (132)

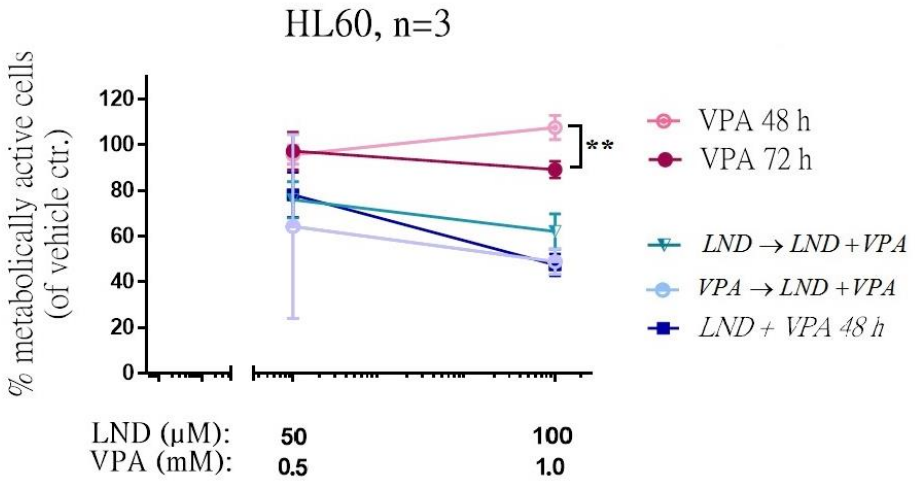

Figure 12. Sequence administration on HL60 cell proliferation of VPA (0.5 mM, 1 mM) alone and in combination with LND (50 µM, 100 µM). The order of administrations were: LND→LND+VPA, VPA→LND+VPA for a total exposure time of 72 hours compared to LND+VPA combined for 48 hours, and VPA alone for 48 and 72 hours. Results are given in means ± SD in triplicate. $**P < 0.01$

To evaluate whether LND works in tandem with VPA, selected concentrations were applied to MOLM13, NB4 and HL60 cells for 48 hours based on single drug treatment results obtained in section 4.2.1 and previous *in vitro* studies on VPA (133). Hoechst 33342 assay provided viability data by the quantitative counting of abnormal and normal nuclear morphology **(Figure 13A,** HL60 shown only**)**. Annexin-V/PI flow cytometric analysis, besides Hoechst 33342 staining **(Figure 13A)** confirmed apoptosis results. Correlation

coefficients were computed to address the association strength between both viability assays. The decrease in viability attained from the combination treatment in both assays correlated well with each other. The correlation coefficients for the strong association between Hoechst 33342 – and Annexin-V/PI viability assay in MOLM13 and NB4 were 0.99 and 0.88 respectively. These data indicated a comparable trend of viability in all three cell lines following combinatorial treatment of VPA and LND **(Figure 13B, C)**. HL60 cells are only presented for Hoechst viability scoring in **figure 13A** since the cells do not expose phosphatidylserine upon apoptosis induction.

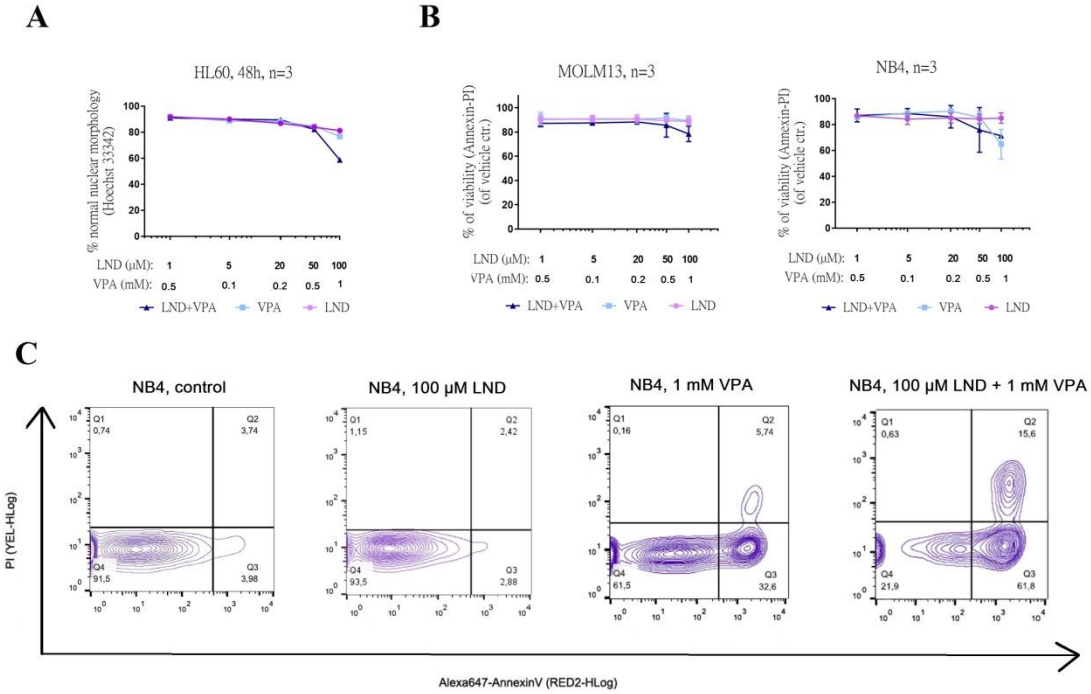

Figure 13. Cytotoxic potentiation by LND (100 µM) when combined with VPA (1 mM) on AML cell lines. Viability was analyzed after 48 hour combination treatment using **(A)** Hoechst 33342 staining (HL60 shown), and **(B)** Annexin-V/PI flow cytometry in MOLM13 and NB4 cells. **(C)** Analysis of viable (AnnexinV-PI-), pre-apoptotic (AnnexinV+PI-), and apoptotic (AnnexinV+PI+, AnnexinV-PI+) is demonstrated with enhanced amount of apoptotic populations of LND (100 µM), VPA (1 mM) co-treatment of NB4 cells.

Anti-proliferative activity following combination treatment with VPA and LND varied among the cell lines **(Figure 14A-C).** An overall higher degree of reduced metabolic activity was observed from three independent studies with MOLM13 **(Figure 14A)** and NB4 **(Figure 14B)** cells thus were suggested being more responsive to co-treatment. However, higher standard deviations across the concentrations (mainly at VPA concentrations ≤ 0.2 mM), contribute to more variance and uncertainty associated with statistical interference of the combination treatment. HL60 cells responded revealed low response to both drugs alone,

resulting in only 10-25 % reduced proliferation when exposed to the highest concentrations of VPA (1 mM) and LND (100 µM), respectively **(Figure 14C)**. Nonetheless, the combined treatment with 100 µM LND and 1 mM VPA reduced the level of metabolically active cells to 47 % in HL60, proposing the evident of a dose-dependent effect. Synergistic induction of apoptosis and reduced proliferation for this dose was demonstrated by the Bliss Independence Model **(Figure 14D)** and calculated for statistical significance by Two-way ANOVA Turkey`s multiple comparisons test (****P*=0.001)**.**

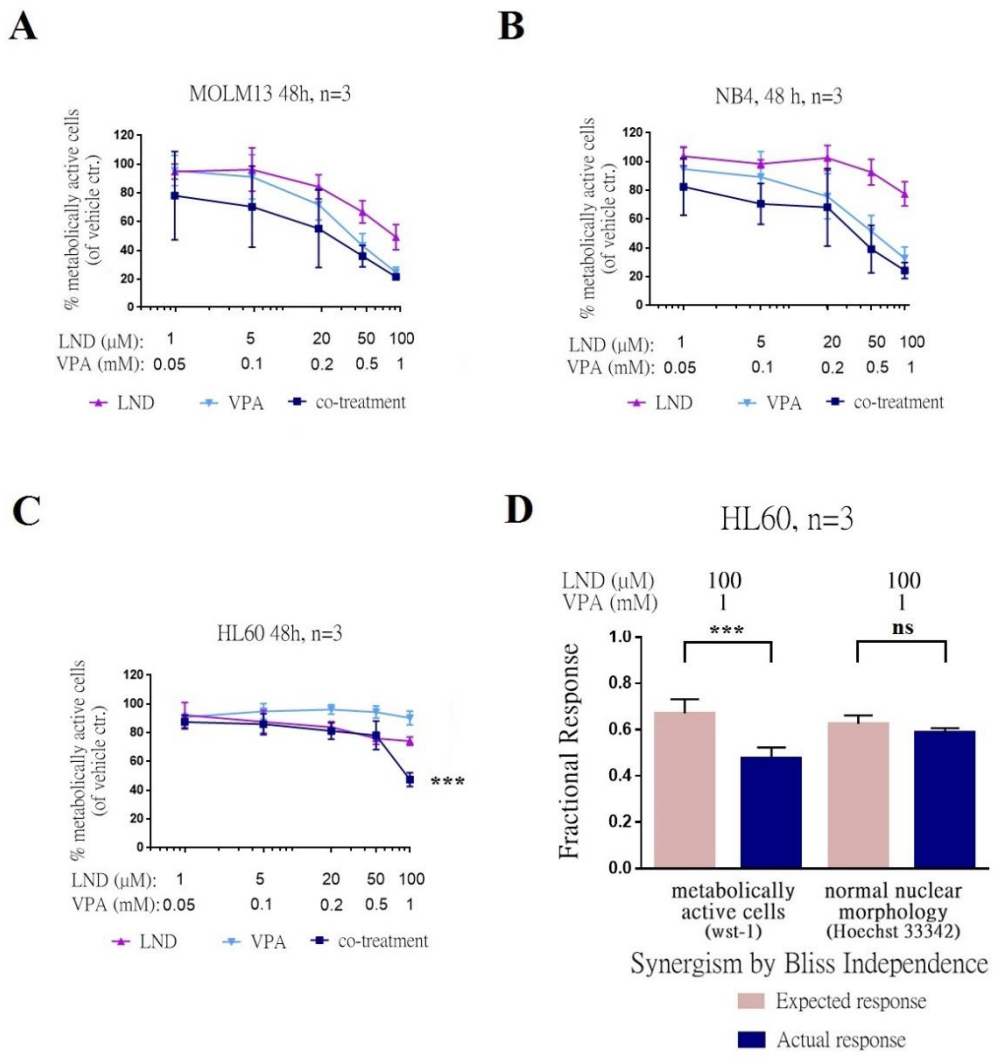

Figure 14. Combinational treatment effect of VPA and LND on cell metabolism and viability of human AML cell lines. Sensitivity for treatment with LND and VPA alone and in combination (actual response) for 48 hours analyzed by WST-1 shown for MOLM13 **(A)** NB4 **(B)** and HL60 cell lines **(C)**. All results are given as mean ± SD for three independent experiments. **(D)** Synergism on viability obtained from Hoechst staining and proliferation inferred by metabolically active cells. Synergistic effect was calculated by Bliss Independence test (expected response) represented in means ± SD in three independent studies on HL60 cells with 100 µM LND combined with 1 mM VPA. p-values calculated by Two-way ANOVA Turkey`s multiple comparisons test (****P* = 0.001)

Since LND has been reported to sensitize other chemotherapeutics (105), it was investigated whether LND could potentiate hydroxyurea (HU) and 6-mercaptopurine (6-MP) that are both been used for therapy in AML patients. (56) The proliferative response following treatment was examined for both combinations. Interestingly LND, seemed to inhibit the effect of HU when combined in HL60 cells **(Figure 15A)**. This was also observed by scoring normal versus abnormal nucleated cells **(Figure 15B)**. Combinational treatment of cells with 6-MP and LND was investigated by proliferative response were the combined effect did not exceed that of either of the drugs alone **(Figure 15C)**.

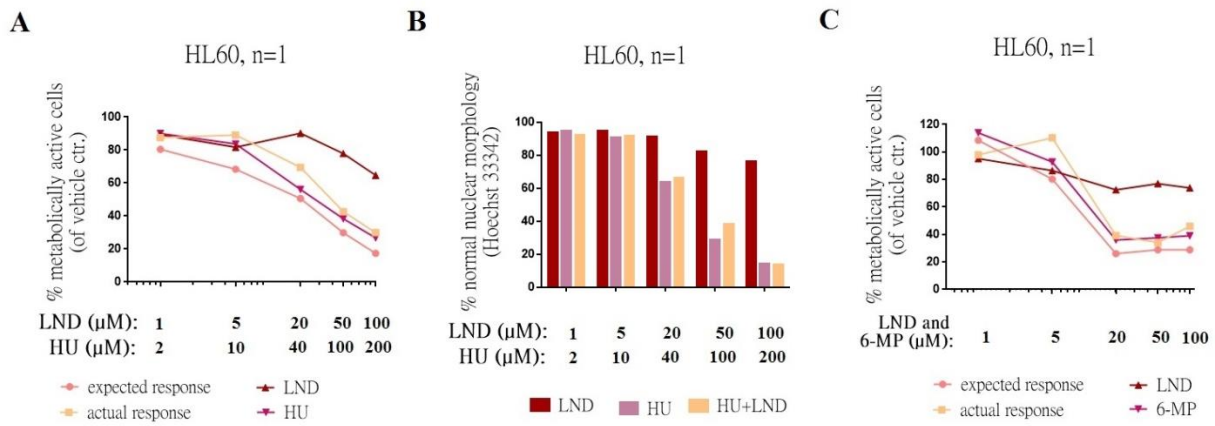

Figure 15. *In vitro* evaluation of LND in combination with HU and 6-MP. Bliss Independence test examined the expected response of the combination treatments (actual response) from one study on HL60 cells (48 h). **(A)** Both proliferation and viability assays assessed an inhibited response of HU when combined with LND. **(B)** 6-MP and LND showed no synergism when combined.

4.2.4 AML Patient cells treated with Lonidamine and Valproic Acid

Drug screening of patient blood samples by proliferation assay was performed to determine drug response and drug sensitivity with LND (1 – 100 µM), VPA (0.05 – 1 mM) alone and in combination treatment for 48 h. AML cells from two AML patients exhibited different degree of sensitivity to the treatment of single drug LND (1-100 µM), VPA (0.05-1 mM) and the combination treatment *in vitro* **(Figure 16)**. Peripheral blood samples, enriched for leukemic blasts by density gradient separation (Lymphoprep), from patient I **(Figure 16A)** showed less response on proliferation to both drugs compared to patient II **(Figure 16B).** Treatment of blasts derived from patient I resulted in an additive anti-proliferative effect by the combination treatment of 50 µM and 0.5 mM. A sample size of one is not substantial for significance testing. However, Bliss Independence model allowed for synergy testing. Bliss Independence model revealed synergism for the combination treatment of 50 µM LND and

0.5 mM VPA on patient I. The expected response in **Figure 16** defines the equation (section 3.12) of the Bliss Independence rule for synergism. Patient II was more responsive to both LND and VPA than patient I, resulting in less metabolically active blasts from peripheral derived blood after treatment. A bone marrow sample was available for patient II, and was treated identically to the blast samples. The cells harvested from the bone marrow showed lower response represented by increased proliferation for all combination doses except 100 µM LND and 1 mM VPA. VPA and the combined treatment followed a similar trend parallel to that obtained in peripheral blood sample, only with an overall increase in proliferation with lower drug response. LND had an enhanced effect on the bone marrow derived sample resulting in 30% less metabolically activity than the peripheral blood sample when treated with same concentration (50 µM). However, PBMC sample **Figure 10A** appeared more resistant to LND than the primary AML patients.

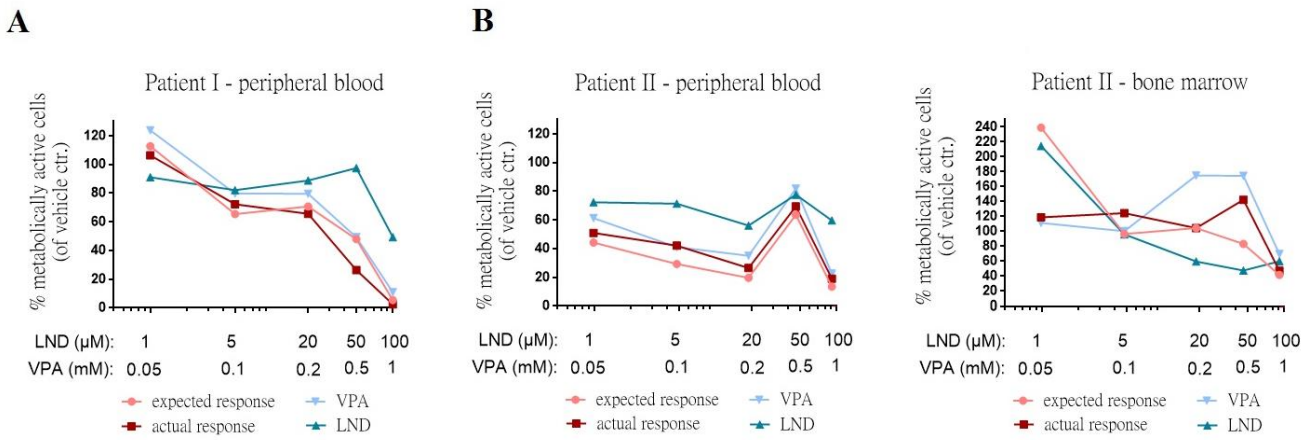

Figure 16. Proliferation changes in AML patient leukoblasts and bone marrow samples treated with LND and VPA. Synergistic effect was calculated by using the Bliss Independence test model (expected response). **(A)** Additive effect of reduced proliferation from the combination treatment with LND and VPA. Synergism indicated when combined with 50 µM LND and 0.5 mM VPA in patient I. **(B)** Sensitivity of peripheral blood sample derived from AML patient II to both agents when treated alone and in combination, but no additive or synergistic effect was specified. Bone marrow derived sample from same patient show greater sensitivity to LND when treated with 50 µM or 100 µM LND alone, or else more resistance to the drugs.

4.2.5 Transient Knockdown of Hexokinase I Potentiating VPA Effect on Proliferation in MOLM13 and NB4 human AML cells

siRNA on HK1 was introduced into HL60, MOLM13 and NB4 cells to investigate if a knockdown of this gene affect the sensitivity of the cell lines to LND (50 µM) and VPA (1 mM) and whether the drugs efficiently inhibit HK1 when present under treatment. The

specificity of LND to inhibit HK1 can to some extent be evaluated by examining whether HK1 knockdown cells treated with LND result in a less effect of anti-proliferation compared to knockdown only. Experiments in HL60 confirmed the LND-dependence of HK1 **(Figure 17A),** were HK1 knockdown cells were less sensitive for LND compared to control transfected cells. Nonetheless, the HK1 siRNA control cells may have responded to the knockdown of HK1 by stimulating proliferation which could be the same response observed in cells treated with LND after knockdown **(Figure 17A)**. No significant change in VPA response was observed after HK1 knockdown in HL60 cells. HK1 knockdown-mediated VPA sensitization may be observed in MOLM13 **(Figure 17B),** but repeated experiments are needed for confirmation. A comparable effect with 80% reduced proliferation was obtained in MOLM13 HK1 knockdown control and in MOLM13 cells with HK1 knockdown and VPA treatment **(Figure 17B)**. **Figure 17C** displays the high SDs from the results in NB4 cells. Together with the already high sensitivity of NB4 cells to VPA, the SDs problematizes the reliability and the actual effect of the knockdown. Normalized data to the consistent controls are presented in **Figure 17 A, B** and **C** for HL60, MOLM13 and NB4, respectively. In MOLM13 and NB4 (P = 0.037*) cells, knockdown of HK1alone potentiated anti-proliferation.

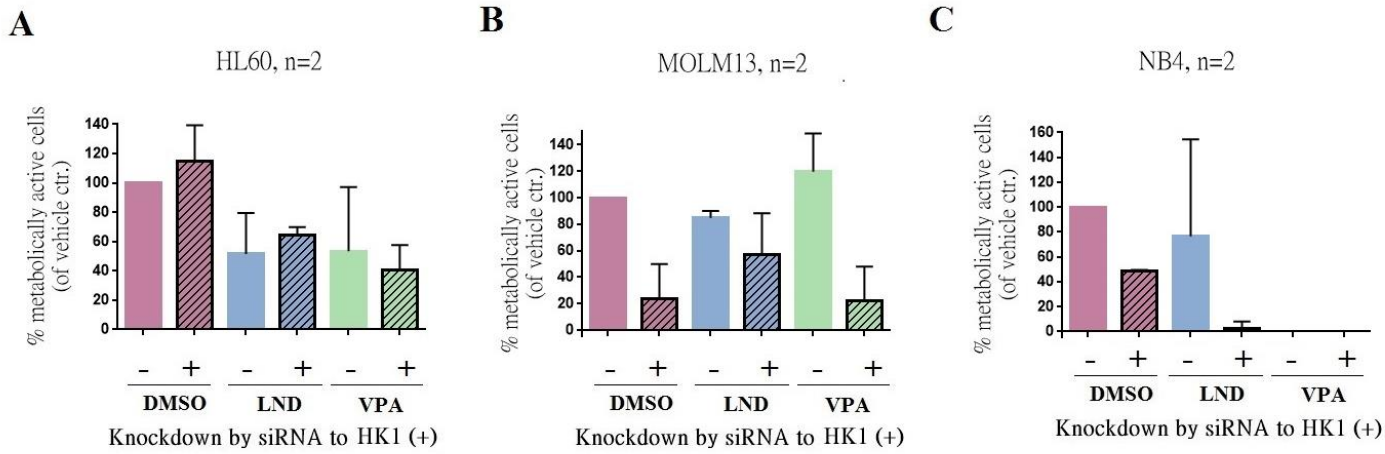

Figure 17. Transient *in vitro* knockdown of HK1 in HL60, MOLM13 and NB4 AML cells by electroporation prior to treatment of LND, VPA or vehicle (DMSO) for 48 hours. The siRNA serving as negative control was AF488 labeled. Two replicates of one study in **(A)** HL60, **(B)** MOLM13 and **(C)** NB4 cells presents the potential of LND and VPA to reduce cell proliferation in non-/ introduced siRNA to HK1. Untransfected samples were normalized to untransfected control, and knockdown (HK1 siRNA) samples were normalized to negative siRNA control (AF488 siRNA). (-) – negative for siRNA, (**+**) – introduced siRNA.

4.3 The effect of Lonidamine and Valproic acid on Hexokinase and other signaling pathway proteins

Western blotting was performed in order to reveal specific proteins and signaling pathways affected by VPA or LND. Phospho-HK1 was shown to be affected by VPA in a previous proteomic study that found reduced protein expression of phosphorylated HK1 in the leukemic cells of VPA treated BNML rats. (3) As LND is not specific to HK1, but is characterized to be an inhibitor of the activity of mitochondria bound hexokinase, the expression level of both HK1 and 2 was investigated. The expression levels of HK2 varied marginally between all lysates within the cell lines. No defined up- or down-regulation could be confirmed, except from a LND treated samples, having to some extent reduced HK2 expression **(Figure 18)**. Protein expression of HK1 was shown to increase in all cell lines after treatment of VPA and the combination of LND and VPA **(Figure 18)**. But as the explored VPA- modulated protein expressions in the BNML-study were phosphorylated, the decreased HK1 expression may only represent a fraction of the total HK1 protein expression in whole cell lysates as observed in this project. Thus the previously observed effect of VPA on HK1 may not be reflected by these western blots. (3) Phosphorylated proteins from cultured HL60, MOLM13 and NB4 cells were therefore purified by affinity chromatography after treatment with VPA or LND. The concentration of the phosphorylated proteins was however not sufficient to permit further evaluation by western blotting.

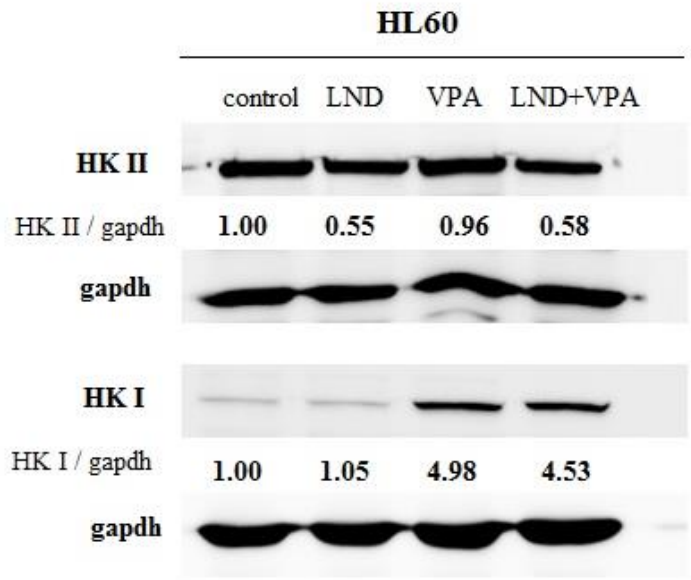

Figure 18. Normalized quantitated data for the compared protein expression of HK2 and HK1. Western detected presence of HK1 and 2 following 48 hour treatment of LND (100 µM), VPA (1 mM)

and the combination of both drugs. Gapdh serves as internal loading control for three independent studies.

In order to assess the functional pathways of LND and VPA in leukemic cells, four other proteins, caspase 9, caspase 8, p21 and pERK1/2 were investigated.

Caspase 9 is cleaved as a step of the initiation of the intrinsic apoptosis signaling pathway, and caspase 8 is cleaved during activation of the extrinsic pathway. These proteins were therefore analyzed as a proof of activation of cell death. **Figure 19 A** shows decreased expression of cleaved caspase 9, and a clear accumulation of cleaved caspase 8 in NB4 cells. MOLM13 treated cells showed similar caspase expression levels, whilst HL60 cells resulted in activation of both apoptosis signaling pathways when treated for 48 hours with 100 µM LND, 1 mM VPA and in combination. P21 is a protein downstream of and under the control of p53. As p21 regulates cell cycle progression by an arrest at G_1/S phase, the expressed level of the protein could indicate whether there is a cell accumulation in the G_1/S compartment following drug exposure. The increase in protein expression of p21 was seen in all cell lines when treated with VPA, with the highest increase in MOLM13 and NB4 **(Figure 19B).** The increase of p21 expression level is supported by previous findings. (134) All cell lines exposed to LND had increased p21 protein expression, however it reduced the large increase induced by VPA when combining the two drugs. ERK signaling pathway frequently operates by negatively regulating apoptosis. Although both VPA and LND have been reported to increase the expression of phosphorylated ERK, combination studies on LND have shown a reduced expression of pERK when working in synergism with other drugs. (103) pERK1/2 protein expression was reduced following 100 µM LND treatment and increased after exposure to 1 mM VPA. The low expression increase by VPA was counteracted by LND when combined **(Figure 19C)**.

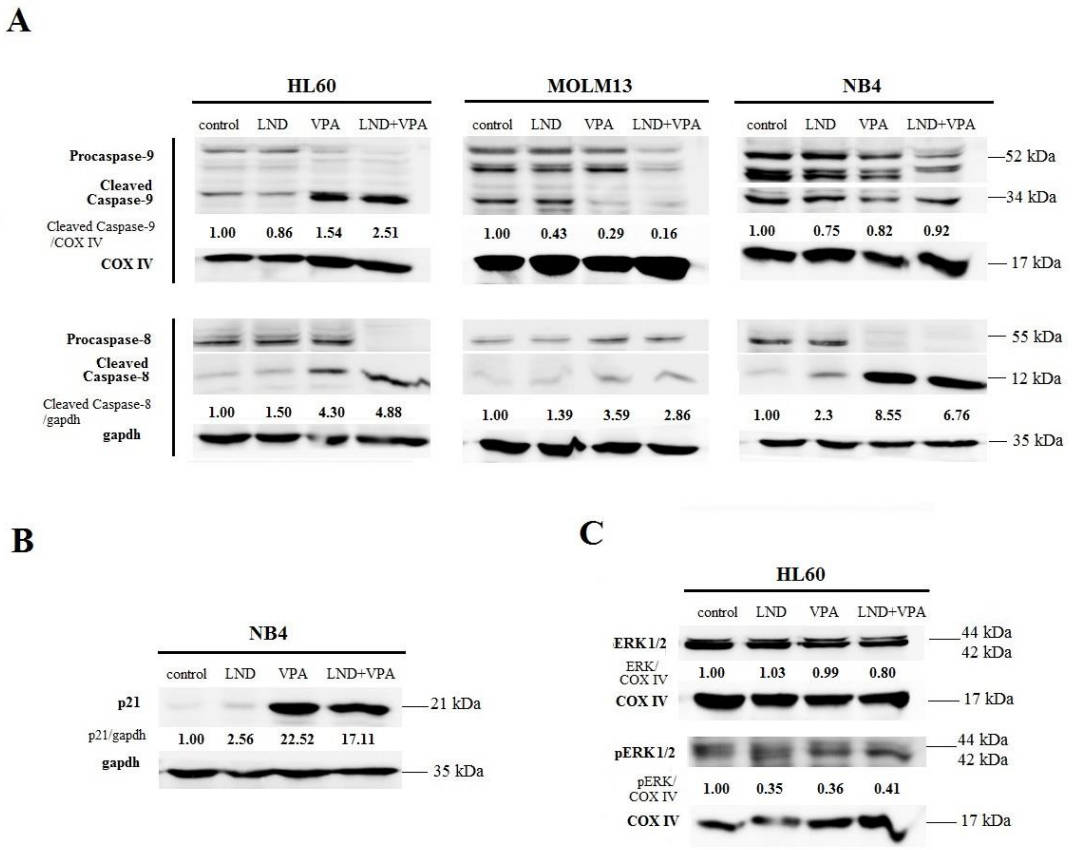

Figure 19. Expression levels of proteins involved in apoptosis regulation and proliferation following LND and VPA treatment. Characterized protein bands were normalized to loading controls (gapdh or cox IV). **(A)** Cleaved form of caspase 9 and caspase 8 present active intrinsic- and extrinsic apoptosis signaling pathways in treated NB4 cells**. (B)** Cell cycle regulatory protein p21 content assessment by quantitative analysis of its protein expression in NB4 cells following treatment. **(C)** Expression of the ERK signaling pathway by phosphorylated ERK1/2 expression in MOLM13 cells.

4.4 Murine MTD study assessing tolerance of selected drug concentrations of Lonidamine

Based on the interesting and encouraging *in vitro* data, a pilot study to determine maximum tolerated dose was performed in NOD/scid/gamma (NSG) mice. Doses were determined based on the literature for evaluating the tolerance of LND. (120) Three female mice received *intra peritoneal* (*i.p*) injections of LND once daily for five days with five day observation**.** Weight was measured every day and the condition of the mice was followed by observation (**Figure 20)**. Injections of 25 mg/kg LND once a day for five days **(Figure 20A)** resulted in approximately 7% weight loss in two mice, whilst the third mouse gained weight by ~ 3%. Nonetheless, the condition of the mice was normal with no visual signs of change in movement and activity. Five minutes after the first injection of 50 mg/kg LND the mice responded with apathy. They moved when disturbed, but quickly resettled. After 24 hours, the

appearance of ruffled fur, dehydration, little movement with quickly resettling, and average weight loss down of 9.61% of total body weight ($P < 0.05$), led to the decision of ending the trial of 50 mg/kg LND dosing **(Figure 20B)**. Subcutaneous injections of 9 mg/mL sodium chloride were administered for one week for recover and weight gain. Because of the high loss of body weight, 25 mg/kg LND was considered as the MTD in this study. The two male NSG mice receiving vehicle only, resulted in no significant weight loss.

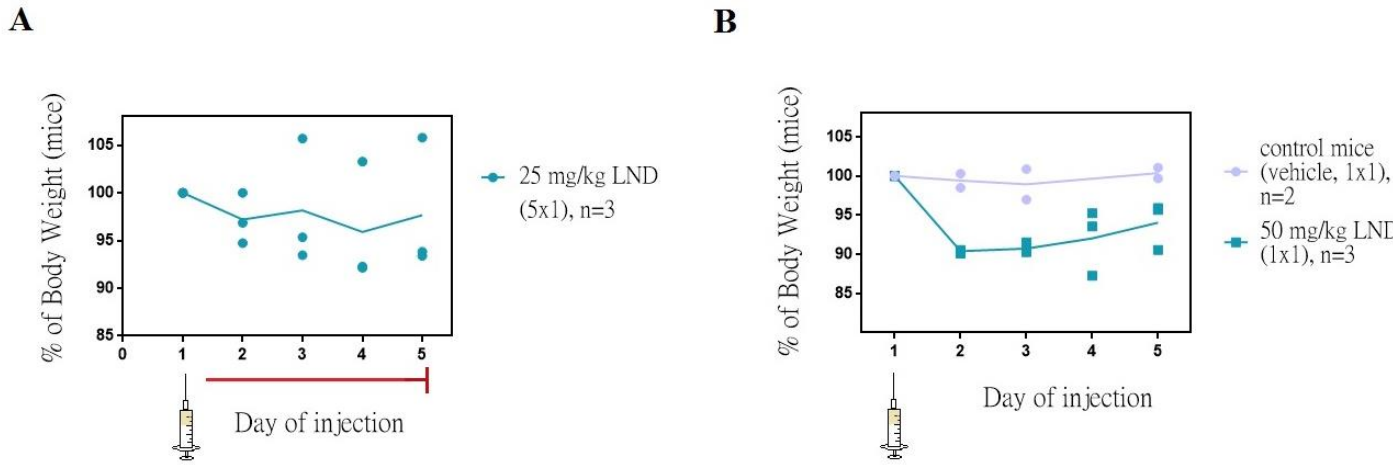

Figure 20. Maximal tolerated dose evaluation of lonidamine in NOD/scid/gamma (NSG) mice. Weight was measured every day and normalized to weight prior treatment, presented as average percentage body weight in graph. Syringe indicates day of *i.p.* injection and the symbols represents variation between mice. **(A)** 25 mg/ml LND administered once daily for five days in three female NSG mice. **(B)** 50 mg/kg of compound reached above the maximum tolerated dose causing toxicity by excessive weight loss close to 10% of body weight. Two male control NSG mice were given vehicle only *i.p.* (10% DMSO, 70% PEG300) for one day.

5. Discussion

In vitro preliminary studies based on metabolism- and apoptosis assays on human AML cell lines treated with either of the drugs LND or MMF enabled us to investigate whether the drugs possess an anti-leukemic potential by themselves and if they enhances that of VPA. Because LND is suggested to selectively inactivate mitochondria bound HK1 and HK2 primarily in tumor cells, one would expect to affect the glycolysis potentially promoting downstream apoptotic activity in AML cells when treated with LND. (100, 135, 136) MMF is a potent inhibitor of IMPDH that has been demonstrated to be a key enzyme of the *de novo* purine synthesis with higher activity in neoplastic cells. (5, 137) The targeted enzymes HK1 and IMPDH are both involved in the signaling pathways that were previously observed to be affected by VPA. (3) For that reason LND and MMF were chosen as investigating agents in a subset of AML *in vitro* studies. As the discovery of those proteins was based on the isolation of leukemic blasts from animals at humane endpoint, further analysis needed to evaluate whether their regulation was of an anti-leukemic effect or a response of resistance to VPA. Consequently, novel *in vitro* drug combination strategies for AML were investigated and evaluated by anti-proliferative and apoptosis assay. Further investigation of the drugs mechanism of action was done by Western blot analysis. Transient knockdown of HK1 and HPRT1 was performed to investigate a more direct inhibition of these proteins, and the potential combination potential with VPA. *Ex vivo* proliferation studies enabled the postulation of drug sensitivity in subgroups of AML patients to LND and MMF.

5.1 Assessing Anti-leukemic Potential of Drug Combinations *In vitro*

Enhanced enzyme activity of IMPDH has previously been linked to increased proliferation in leukemic cells. (87) Given that glutamine is an essential fuel for cancer cell metabolism where purine synthesis is dependent on this nutrient and that IMPDH is the rate limiting enzyme of the *de novo* guanosine synthesis, we hypothesized that the potential of the semisynthetic drug MMF to inhibit IMPDH may possess an additional anti-leukemic effect when combined with VPA. The human AML cell lines HL60, MOLM13 and NB4 selected to represent varying subgroups of patients in the heterogeneous disease AML indicated sensitivity by proliferation and viability assays to MMF. IC_{50}s found in this project **(Figure 2D-F**) are comparable to those found by *Zeevi et al*. in human T lymphoid (MOLT-4, IC_{50} = 365 nM), human B lymphoblasts (EB-DN, IC_{50} = 292 nM), and AML cell line (HL60, IC_{50} = 365 nM). (138) It is

however obvious that the different cell lines show differences in drug sensitivity when comparing IC_{50} values, suggesting a similar variability could be found in AML patients.

Preliminary results for comparing the metabolic activity of normal healthy lymphocytes and AML leukemic blasts **(Figure 4)** showed a high variance between patient responses, but that PBMCs in general tolerated MMF well, with increased proliferation. MOLM13 (IC_{50} 0.048 µM, **Figure 2E**) as well as Patient 2 showed higher sensitivity to MMF compared to healthy lymphocytes and the AML cell lines HL60 and NB4. (139) Both HL60 and the APL cell line NB4 need higher concentrations (0.307 µM and 0.103 µM, respectively) of MMF, to reach half of the maximal inhibitory concentration **(Figure 2D, F)**. Nonetheless, the maximal inhibited response (bottom plateau in **Figure 2F**) was slightly higher in NB4 cells than HL60 and MOLM13 by doses investigated. Thus MMF may have a greater potential in the APL subtype of AML patients at concentrations higher than 100 nM MMF, but at these concentrations MMF may not have high enough specificity relative to diseased cells. All IC_{50} concentrations **(Figure 2D – F)** are therapeutically attainable concentrations (0.1 – 10 µM). (140) However, within the limited time constraints and the interest in proceeding with experiments investigating MMFs` attribute in combinational therapy, only two replicates were performed. Thus, for statistical evaluation additional experiments will be needed.

5.1.1 Apoptosis induction by MMF

The effect of MMF in AML cells obtained from WST-1 proliferation based assay is assumed to be of cell growth inhibition since all three AML cell lines tested in this project showed metabolic inhibition, and hematopoietic cells depend on the *de novo* guanosine synthesis for replicating. However, MMF also induced fragmented nuclear morphology in all three cell lines (0.05 µM and higher) investigated. **Figure 3B** shows slightly higher levels of abnormal nuclear morphology in HL60 at higher concentrations (1 µM) compared to MOLM13 and NB4. In the two latter cell lines, condensed nuclear morphology dominates over the incidence of fragmented nuclei at 0.05 µM MMF, especially in MOLM13 (data not shown). To verify that the nuclear morphology assay indicated apoptosis, Annexin-V/PI flow cytometric analysis was performed. As HL60 does not expose phosphatidylserine extracellularly during apoptosis, (141) Annexin-V cannot be used to label this cell line. Flow cytometric analysis was therefore performed only on MOLM13 and NB4. The decrease in percentage of metabolically active MOLM13 and NB4 cells was not reflected in a similar decrease in viability by Annexin-V/PI, displayed by **Figure 5A/C**. The lower metabolic activity found by

WST-1 conversion in NB4 cells can be due to cell cycle arrest as a response to MMF as a large fraction of the cells also show abnormal nuclear morphology and apoptosis by flow cytometry (MMF, **Figure 5**). The treated NB4 cells at these concentrations are therefore measured as less apoptotic cells by Annexin-V, which may clarify the difference between the results from the metabolism- and viability assay. There is a slightly larger population of viable cells (Annexin-V positive) in MMF treated MOLM13 cells accompanied with lower levels of metabolically active cells to concentrations between 0.1 – 0.5 µM MMF. If these experimental results on MOLM13 cells can be reproduced, they may propose the assumption that low concentrations of MMF induce cellular dormancy but not apoptosis, whereas the reduced metabolic activity at the two higher doses is due to the cells being apoptotic. (142) The same can be found for NB4.

5.1.2 No enhanced anti-leukemic effect from the combination treatment of MMF and VPA

The *salvage pathway* of guanosine synthesis is to some extent unimportant for T- and B-lymphocytes. (139) However, about 90% of purines are recycled by the *purine salvage pathway* in humans, thus being still important in other cells. (143) Since VPA treated BNML rats showed to have reduced the expression levels of phosphorylated HPRT1 when at late stage of the disease, the influence of HPRT1 on leukemic blasts became an interesting topic to investigate. Thus VPA and MMF were combined for treatment. The combination of MMF with VPA in human AML cells is novel. Sodium valproate and MMF has previously been investigated in three renal allograft recipients where valproate was given for seizures. (144) In this trial the concentration of MPA in blood decreased in all recipients when concomitantly receiving sodium valproate. An increase of 71.4% of the dose was required to maintain the area under curve concentration (AUC) of MPA. We found no cooperative effect of the combination treatment with MMF and VPA when analyzing for metabolically active or viable leukemic cells, on the other hand metabolic activity of cells treated with MMF or MMF combined with VPA was more or less identical. However, in **Figure 5C** the percentage of viable MOLM13 cells analyzed by Annexin-V/PI flow cytometry indicates that VPA possibly can influence the viability effect of MMF by decreasing its cytotoxicity when combined at lower concentrations (0.25 - 1 µM MMF, 0.25 – 1 mM VPA).

5.1.3 Alternative Combination Treatments with MMF

Other combination strategies were investigated briefly for MMF. As the purine *salvage pathway* also contain the adenine phosphoribosyl transferase (APRT) **(Figure 1)** whose activity was associated with an increase in AML patients in the study by *Davidson* and *Winter*. (56) MMF was combined with the cytotoxic urea analogue hydroxyurea (HU) that inhibits the ribonucleotide reductase. (145) This combination treatment **(Figure 7A)** showed no additional effect on reduction of metabolic activity. Analysis of an imbalance in ribonucleotide pools by for example purine nucleotide separation by liquid chromatography could assess a better prediction of the particular nucleotide concentrations following treatment. (145) LND has been reported to increase the cytotoxic effect of conventional anticancer agents such as doxorubicin, methotrexate, and etoposide in human and murine fibrosarcoma cell lines, but also in other combinations in leukemic cells. (105, 110, 111) These chemotherapeutics induce oxidative stress. Lopez-Lazaro observed that for inhibition of glycolysis in cancer cells to be efficient, additional drugs affecting the production of ROS, H_2O_2 in particular, would be needed to utilize the hypothesis of the Warburg effect in the treatment of cancer cells. (146) As both inhibition targets HK1 and HPRT1were found to be down-regulated in an AML study, the combinational effect of both agents was briefly investigated by WST-1. (3) An enhanced potentiation was however not observed by the combination treatment **(Figure 7B)**.

5.1.4 Investigated potentiation by LND of other chemotherapeutics to induce apoptosis and metabolic inhibition

The anti-leukemic effect on reducing blast metabolic activity and inducing cell death using LND as monotherapy was modest in HL60, MOLM13 and NB4 cells (**Figure 9, 10**) in a dose- and time dependent manner. This has also been reported for the sensitivity to VPA. (133) Synergism between the two drugs was discovered for HL60 cells in both metabolic- and Hoechst 33342 nuclear morphology assays (**Figure 14D**). Sequence administration of LND and VPA was conducted and resulted in compliance to the assumptions of the need for longer incubation time and dose dependency for synergistic effect (**Figure 12**). From this, it appears that TP53 depleted blasts might be more responsive to LND, in a dose dependent manner compared to cell lines with p53 wild type expression. LND may induce its effect in a p53 independent manner which can be supported by other findings. (106) Enhanced proliferation of NB4 cells was seen at concentrations lower than 100 µM LND **(Figure 10A).** The finding

that low or median doses of a drug might increase proliferation has previously also been for VPA in a subset of primary AML leukemic cells treated *ex vivo*. (147)

The two drugs 6-mercaptopurine (6-MP) and hydroxyurea (HU) are often used in palliative treatment and in older AML patients, but are not associated with sufficient survival outcomes. (148) The potential of LND for sensitizing cells to drugs may ensue by increasing the efficiency of 6-MP and HU, and was therefore explored **(Figure 15)**. The pilot study showed the combinations to be of no beneficial effect on metabolic activity. The antimetabolites 6-MP and HU were the dominating drugs leading the cytotoxic effect of the combination with LND. Interestingly, the latter combination seemed to induce less growth inhibition in HL60 cells than with single drug treatment. The difference between expected additive effect (Bliss Independence test) and actual combinatorial effect is however low, and as this experiment was performed only once, it is likely that a repeat of this study might result in the loss of this effect due to experiment-to-experiment variation. Sub-G1 peaks in LND treated HL60 cells in a previous study may support this finding suggesting LND to protect the cells from HU induced S phase arrest, which could be an antagonistic effect also observed by Hoechst viability assay. (149) These results should be repeated for a more reliable evaluation.

5.2 Distinct response to VPA and LND in native AML peripheral blood versus bone marrow

In the primary AML cell experiment with patient derived blasts described in section 4.2.4, cells from patient II appeared more sensitive to VPA at lower concentrations and to LND at concentrations up to 20 µM, than cells from patient I. But they both follow a similar trend where the decrease in percentage of metabolically active cells was lesser at higher drug concentrations compared to the decrease in metabolically active cells at lower concentrations of both drugs LND and VPA. Thus, higher concentrations of the agents may not be needed to achieve response on decreasing the rate of cancer growth in these specific patients. Unfortunately, resistance to VPA was observed in the bone marrow derived sample comparable to the peripheral blood sample from the same patient (II), whilst an enhanced sensitivity to LND was observed. More statistically-valid and quantitative analysis is needed for reliable interpretations to be made. However, distinct phenotypes in for example adhesion molecule cell surface expression between blood and bone marrow derived from same patient, is a subject of increasingly intense investigation. (150)

5.3 Validation of HK1 and HPRT1 transient knockdown effecting the metabolically activity in HL60, MOLM13 and NB4.

Due to time constraints, knockdown of HPRT1 was only performed in HL60. The knockdown did not affect the measurable effect on metabolic activity in the control (DMSO) nor did it increase the effect of MMF suggesting the reduction of HPRT1 alone not to be sufficient to affect metabolic activity. Consequently, the effect seen by MMF may not preferably be due to inhibition of HPRT1. However, HPRT1 knockdown seemed to sensitize HL60 cells to VPA. If this finding can be verified by repeated studies, it may demonstrate that a more direct targeting of HPRT1 indeed can increase the responsiveness to VPA. The consideration of combining VPA with a different drug with higher specificity to HPRT1 than what MMF seems to possess, could potentiate VPA as an anti-leukemic agent in AML patients. (151)

The effect of knockdown of HK1 in HL60 cells did not seem to have a distinguishable effect on metabolic activity (**Figure 17A**). Comparing the results obtained from HL60 with those obtained in MOLM13 and NB4 cells (**Figure 17B**, **C)**, knockdown of HK1 showed to induce growth inhibition in control cells in both cell lines. HK1 knockdown in MOLM13 enhanced the sensitivity of VPA and LND, however the results for VPA and control cells were similar suggesting no additional effect was obtained by combining VPA and HK1 depletion. For NB4, variations in LND treated cells not subjected to HK1 siRNA, as well as the high sensitivity for VPA meant no conclusions could be drawn. Whether the potential increased effect of LND and VPA by HK1 knockdown found in MOLM13 is due to a decrease in number of cells or that the cells present are less metabolically active is difficult to say when not combined with additional assays, for example Hoechst viability assay gives an impression on whether the reduced fraction can be due to apoptosis induction, in other words fewer cells. Because of the potential sensitizing effect of VPA by HK1knockdown in MOLM13 and HPRT1 knockdown in HL60, this might suggests that the reduced protein expression observed from the VPA treated BNML rat study were of an anti-leukemic effect and not a resistance response aiding in disease progression. However, sample size needs to be increased for a significant evaluation.

Microscopy was used for the evaluation of transfection efficiency by the examination of AF 488 positive cells. But since siRNA was still present in the cell suspension, causing high background, the distinction between AF 488 positive and negative cells was not obtainable.

Hence quantification of positive versus negative transfected cells was not performed. Nonetheless, knockdown was assumed to be induced as a difference in VPA +/- HPRT1 siRNA was observed **(Figure 8)** and for MOLM13 and NB4 +/- HK1 siRNA **(Figure 17)**. If HK1 and HPRT1 are involved in mediating the growth inhibitory effect of LND and MMF, respectively, we would expect less sensitivity to LND and MMF in the knockdown cells because their proliferation would be less dependent on HK1 and HPRT1. The results obtained in this project **(Figure 8 and 17)** comprise great variation which would need replicative studies to clarify whether there is an actual decreasing or increasing sensitivity to LND and MMF by HK1 and HPRT1 knockdown. However, from these preliminary results, HK1 does not seem to be the only inhibitory mediator of LND anti-leukemic effects in HL60 and MOLM13 cells, while HPRT1 does not seem to be pivotal for an anti-proliferative effect of MMF in HL0 cells.

5.4 The effect of Lonidamine and Valproic acid on Hexokinase and other signaling pathway proteins

The ability of VPA to induce apoptosis, cell differentiation and inhibition of proliferation and cell cycle progression is suggested to be important for its cytotoxic effect. Nonetheless, VPA may also increase superoxide formation as it prevents the flow of electrons through the electron transport chain by interacting with biological components such as for example superoxide dismutase. (151) The influence of oxidative phosphorylation may obscure the results from the conversion of WST-1 salt to formazan, causing the varying measurements from the proliferation assay which can be clearly observed in **Figure 5A**. However, the inhibition of HDACs by VPA affects several downstream mechanisms of differentiation, cell growth, and apoptosis. (52) The active signaling pathways in AML after a response by VPA treatment in the BNML rat model revealed a reduced expression of HK1. Given that the rats with leukemia responded to the treatment and that overexpression studies have implicated pro-survival role of HK1, we hypothesized that the protein expression of phosphorylated HK1 would be reduced by VPA in human AML cells lines and may contribute to increase the anti-leukemic effect of VPA. (3, 152) However, **Figure 18** shows that this was not the case in HL60, MOLM13, and NB4 AML cells when characterized by Western blotting. We did not expect to obtain less expressed HK1 from LND treated samples since LND inhibits this enzyme activity and not in particular affects HK1 by reducing its protein expression. As the extracted proteins from moribund rats were purified for phosphorylated proteins through

affinity chromatography, this was repeated in this project in the attempt to reproduce the effect seen *in vivo* with VPA, only with human AML cell lines *in vitro*. However, phosphorylated protein concentrations that remained after purification procedure were too low for further investigation of the extent of phosphorylation by separation on Western blot. Thus the determined protein content detected by Western blotting **(Figure 18)** presented in this thesis represents total HK1 protein, and not only the phosphoproteins, suggesting that the protein expressed do not have to be biological active. However, studies have shown that the detachment of HK1 from VDAC1 proceeds apoptosis. (153) Thus, cytosolic and mitochondria fractions of cells could be separated after treatment and investigated for their fractions of HK1 to provide a closer estimation of active HK1 versus non-active HK1. The *in vitro* results on HK1 protein expression in this thesis were based on 48 hour treatment, whilst the BNML rats were treated with VPA for four weeks (five days a week). Thus, the increase of protein expression observed might be a consequence of compensation for the inhibitor-mediated decrease in HK1 that could act as a regulating factor for the expression of HK1. Since HK2 also is said to be inhibited by LND, its expression was studied by Western blotting. (135, 136) Less differences in HK2 protein expression in treated with LND and VPA was shown for HK2 than for HK1. As the antibodies used for detection of HK1 and HK2 were not specific for the phosphorylated HK1 and HK2, it is not sure if the expressed proteins resemble the actual HK1 and HK2 activity in cells. Nonetheless, the results indicate that the total amount of HK2 does not change when exposed to VPA or LND.

The major players of the signaling pathways in apoptosis are a group of zymogenic cysteine proteases (caspases). (154) They are present in the cell in an inactive form when not stimulated by either the death receptor pathway by tumor necrosis factor family: the extrinsic pathway for programmed cell death, or by the mitochondria mediated intrinsic pathway. Pro-apoptotic agents inhibiting HK1 and HK2 binding to VDAC1 on B-cell chronic lymphocytic leukemia was showed to activate the mitochondrial pathway by releasing cytochrome c to the cytoplasm. (155) Subsequent involvement of apoptosome formation and activation of the initiator caspase 9 does normally proceed. And as previously explained in section 1.5.3, the intrinsic caspase-mediated apoptotic pathway may be escaped at abnormal hexokinase binding to VDAC1. **Figure 19A** and quantitative analysis of protein expression through Western blotting indicate the opposite downstream signaling from what is proposed by the literature where LND is supposed to induce mitochondrial apoptotic signaling pathway. Only the addition of VPA alone or combined with LND treated HL60 showed increased expression

of cleaved caspase 9 **(Figure 19A)**. The increased intrinsic apoptosis induction through enhanced protein expression levels of cleaved caspase 9 can be reflected by the synergistic effect as a consequence of inhibited metabolism in HL60 **(Figure 14C)**. Diminished expression of cleaved caspase 9 expression following treatment of LND or VPA (MOLM13, NB4) may suggest the prevention of apoptosome formation. AKT and ERK are two key targets for therapeutic intervention as they are commonly active in acute myeloid leukemia. They are two kinases that can subsequently inhibit the enzymatic activity of caspase 9 through phosphorylation. (104, 156) Furthermore, the expression of ERK has been shown to be enhanced in VPA treated endothelial cells, supporting the increased expression of phosphorylated ERK1/2 in **Figure 19C**. (104) The reduced expression of phosphorylated ERK1/2 after treatment with LND may not be adequate to dismiss the possibility that LND rather provoke activation of ERK kinase, as previously been observed, but which was attenuated when combined with arsenic trioxide. (103) Co-treatment of LND and VPA reduced the protein expression on phosphorylated ERK1/2 beyond what was obtained when treated with VPA alone. The initiator caspase 8 of the extrinsic apoptosis signaling pathway was clearly detected in its cleaved form **(Figure 19A)** suggesting for TNF stimulation and mediated apoptosis though the extrinsic signaling pathway. The pro-apoptotic stimulation of TNF-α is an effect that has already been observed to be specific to VPA by *Wang et.al*. (157) This increased expression of pre- apoptotic inducing proteins can be recognized by the apoptotic populations formed following treatment shown by flow cytometric analysis **(Figure 13)**. To determine whether all three drugs, MMF, LND and VPA induce apoptosis rather than necrosis in the susceptible cells, a DNA ladder assay could be performed.

The increased expression of $p21^{WAF1/CIP1}$ can be supported by other literature reporting it to be modulated by VPA. (55) p21 can induce cell cycle arrest in VPA treated cells which does not appear to be p53-dependent, but rather likely due to changes in histone acetylation at the promoter of p21. (158) This observation is compatible with the WST-1 proliferation assay result described in section 4.2.3, showing an independent response in LND and VPA treated TP53 depleted cells **(Figure 14C)**. Furthermore, increased $p21^{WAF1/CIP1}$ expression could indicate an arrest in cell cycle progression at G_1 and S phase. Detailed investigation of p53 mediated mechanisms in response for LND-induced effect was beyond the purpose of this project. The validation of the suggested cell cycle arrest at G_1/S phase could be analyzed by flow cytometry using propidium iodide DNA staining.

5.5 Preclinical toxicity in mice determined the maximum tolerated dose and its toxicity

The preliminary maximum tolerated dose (MTD) study was performed to evaluate the safety of LND and assess the optimal dosing for subsequent therapies. The literature available described previously used doses at experimental procedure, ranging from 50 mg/kg to 100 mg/kg once daily. (159, 160) The route of drug delivery in this thesis was intraperitoneally, same as in the literature mentioned. The drug has a low solubility in water, thus may precipitate in stomach before absorption when given orally. Because of this low solubility, a higher percentage (70%) of the vehicle consisted of PEG300, but was considered safe to use confirmed by administering of vehicle only in two control mice. (161) The primary dose at 50 mg/kg/day was supposed to be the lowest dose of the planned doses administered in this study (50 mg/kg, 75 mg/ and 100 mg/kg). But 5 minutes after first injection they already appeared lethargic as they did not move around in cage and quickly resettled when disturbed by opening of the cage. Following 24 hours, an unacceptable toxicity was observed by weight loss of 9.61% (average of three mice) **(Figure 20B).** Ruffled fur due to piloerection and loss of body weight were signs assumed to be due to dehydration mimicking LND interference with mitochondria function, affecting the energy metabolism by inhibition of cellular respiration. For a quick recover 0.9% sodium chloride solution was administered subcutaneously. The dose was reduced to 25 mg/kg/day LND, which resulted in weight loss of just above 7-8% **(Figure 20A)** and no signs of phenotypic toxicities. Since LND is intended to be combined with VPA in mice bearing subcutaneously implanted leukemia cells, the study was not continued to reach fully 10% loss in body weight. Whether LND at 25 mg/kg/day is of true therapeutic advantage can be assessed in further studies with tumor studies in mice. However, this study showed that the MTD of *i.p*. administered LND is 25 mg/kg for female mice over a period of 5-day dosing and is safe to mice with no observable side effects. The MTD in this study was lower than what had previously been used in the literature that we based our doses on. But in one of the studies the mice died right after completed 3 hour experiment (100 mg/kg). (162) An anti-cancer effect of concentrations with LND < 50 mg/kg has been observed, but with only few experiments performed. (163)

5.6 Conclusions and Future perspectives

The *in vitro* metabolism inhibiting effect of MMF indicated that the drug may have a role in the treatment of AML, but the need for combination treatment is apparent for an enhanced

efficiency among AML patient samples. Nonetheless, no toxic effect on PBMC metabolism was obtained. LND exhibited modest cytotoxicity against all AML cell lines tested in this thesis. Significant synergistically inhibited metabolism in HL60 cells was demonstrated *in vitro* by WST-1 assay and supported by reduced pERK1/2 expression through Western blot analysis, suggesting that combination of HDACi VPA with HK1 inhibitor LND could be beneficial in the treatment of AML expressing depleted p53, and is to our knowledge the first report of LND and VPA combination efficacy in AML study. A pilot preliminary toxicity study showed 25 mg/kg/day for 5 days of LND in NOD/scidILrgamma female mice through *i.p.* administration to be well tolerated. These data may assist in the design and interpretation of additional preclinical investigations of LND combined with VPA in mice with subcutaneously implanted leukemic cells.

To not wrongly interpret the anti-proliferative effect observed by MMF and LND treatment, measurement of the tritiated thymidine (^{3}H) incorporation should be considered as a more specific method for the evaluation of cell proliferation. This will also be important since WST-1 conversion by cellular oxidoreductase activity can differ among cell lines due to varied extracellular superoxide content and by the interference of VPA in the formation of ROS. Besides, the examination of the cells` stage of differentiation should be assessed by immunophenotyping. It would also be interesting to mimic the conditions in the leukemic bone marrow by modified culture medium reflecting the concentrations of key metabolites found in bone marrow and explore whether experiments under hypoxia (2% O_2) show other results from combination treatment.

Inhibition of cancer cells' favor of accumulating energy production by cytosolic glycolysis for the anabolic processes may be shunted towards other energetic processing pathways such as catabolic oxidative pathways within the mitochondria. Thereby might driving cancer cells on glutamine dependency, regulated by c-myc which again, according to The Champion ChiP Transcription Factor Search Portal, regulates the transcription of HK1. However, AML blasts holding isocitrate dehydrogenase (IDH) mutations would likely benefit of a shift towards mitochondria respiration with glutamine metabolism as IDH mutations result in enzyme activity utilizing glutamine to its profit for cancer growth induction. (73)

We have sought to determine signaling cascades mediated by LND that sensitizes leukemic blasts to other chemotherapeutic agents when combined. Plausibly and also demonstrated by

other studies, is the greater extent of inhibition of HK1 and HK2 by LND related to an elevated aerobic glycolysis. (164) This hypothesis can however not be reflected by the comparison of HK1 and HK2 protein expression level by Western blot analysis **(Figure 15)** and growth inhibition **(Figure 7A)** as the protein expression level increased with enhanced anti-metabolic activity effect. Treating IPC-81 cells derived from the BNML rat model followed by immobilized metal affinity chromatography (IMAC) prior to investigation of HK1 expression level by immunoblot or 2-dimensional gel-electrophoresis, exposing the altered isoelectric point of the phosphorylated proteins, could closer reflect the experimental finding of reduced expression of HK1 in the BNML-study.

For future combination experiments it would be interesting to see whether the effect on inhibition of cytosolic glycolysis energy production by LND could be utilized in the advantage of a cytotoxic effect when combined with a H_2O_2 producing agent such as for example Bortezomib that is well tolerated in elderly patients. (165) As a prominent result in this work, we demonstrated that HPRT1 and HK1 can have a pivotal role in sensitizing VPA in AML cells. This was particularly demonstrated by HPRT1 knockdown in HL60 cells and HK1 knockdown in MOLM13 and NB4 cells, for VPA treatment. Quantitative real-time PCR (qRT-PCR) and Western blot could be used for the evaluation of a successful knockdown or not. Nonetheless, we speculate that the ability of VPA to induce cell growth inhibition is likely to be potentiated by the combination of VPA with more specific HK1 and HPRT1 targeting drug. The quantification of HK1 and HPRT1 after transient knockdown should be validated by Western blot analysis. Furthermore, siRNA knockdown to HK1 and HPRT1 in PBMCs will reveal whether this strategy can be feasible in multicellular organism.

References

1. Estey E, Dohner H. Acute myeloid leukaemia. Lancet. 2006;368(9550):1894-907.
2. 5%-Year Relative and Period Survival by Race, Sex, Diagnosis Yeas and Age [Internet]. The National Institute of Health. 2011. Available from: Available from: http://seer.cancer.gov/csr/1975_2011/browse_csr.php?sectionSEL=13&pageSEL=sect_13_table.16.html.
3. Forthun RB, SenGupta T, Skjeldam HK, et al. Cross-Species Functional Genomic Analysis Identifies Resistance Genes of the Histone Deacetylase Inhibitor Valproic Acid. PLOS One. 2012;7(11):e48992.
4. Floridi A, Lehninger AL. Action of the antitumor and antispermatogenic agent lonidamine on electron transport in ehrlich ascites tumor mitochondria. Archives of Biochemistry and Biophysics. 1983;226(1):73-83.
5. Majd N, Sumita K, Yoshino H, et al. A Review of the Potential Utility of Mycophenolate Mofetil as a Cancer Therapeutic. Journal of Cancer Research. 2014;2014:12.
6. Hortobagyi GN. Anthracyclines in the treatment of cancer. An overview. Drugs. 1997;54 Suppl 4:1-7.
7. Tefferi A, Letendre L. Going beyond 7 + 3 regimens in the treatment of adult acute myeloid leukemia. J Clin Oncol. 2012;30(20):2425-8.
8. Kantarjian H, Ravandi F, O'Brien S, et al. Intensive chemotherapy does not benefit most older patients (age 70 years or older) with acute myeloid leukemia. Blood. 2010;116(22):4422-9.
9. SEER Stat Fact Sheets: Acute Myeloid Leukemia (AML) [Internet]. Surveillance, Epidemiology, and End Results Program. Available from: http://seer.cancer.gov/statfacts/html/amyl.html.
10. Chauncey TR, Rankin C, Anderson JE, et al. A phase I study of induction chemotherapy for older patients with newly diagnosed acute myeloid leukemia (AML) using mitoxantrone, etoposide, and the MDR modulator PSC 833: a southwest oncology group study 9617. Leuk Res. 2000;24(7):567-74.
11. Appelbaum FR, Gundacker H, Head DR, et al. Age and acute myeloid leukemia. Blood. 2006;107(9):3481-5.
12. Turgeon LM. Clinical Hematology Theory and Procedures. 5th edition ed. Sabatini P, editor2012. 612 p.
13. Dohner H, Estey EH, Amadori S, et al. Diagnosis and management of acute myeloid leukemia in adults: recommendations from an international expert panel, on behalf of the European LeukemiaNet. Blood. 2010;115(3):453-74.
14. Vardiman JW. The World Health Organization (WHO) classification of tumors of the hematopoietic and lymphoid tissues: an overview with emphasis on the myeloid neoplasms. Chem Biol Interact. 2010;184(1-2):16-20.
15. Knudson AG. Hereditary cancer: two hits revisited. J Cancer Res Clin Oncol. 1996;122(3):135-40.
16. Shen Y, Zhu YM, Fan X, et al. Gene mutation patterns and their prognostic impact in a cohort of 1185 patients with acute myeloid leukemia. Blood. 2011;118(20):5593-603.
17. Shih AH, Abdel-Wahab O, Patel JP, et al. The role of mutations in epigenetic regulators in myeloid malignancies. Nat Rev Cancer. 2012;12(9):599-612.
18. Plass C, Oakes C, Blum W, et al. Epigenetics in acute myeloid leukemia. Semin Oncol. 2008;35(4):378-87.
19. Kakizuka A, Miller WH, Jr., Umesono K, et al. Chromosomal translocation t(15;17) in human acute promyelocytic leukemia fuses RAR alpha with a novel putative transcription factor, PML. Cell. 1991;66(4):663-74.

20. Duffield AS, Aoki J, Levis M, et al. Clinical and pathologic features of secondary acute promyelocytic leukemia. Am J Clin Pathol. 2012;137(3):395-402.
21. Karen W.L. Yee ea. Older patients with acute myeloid leukemia. 2010;6(3):774.
22. Kumar CC. Genetic Abnormalities and Challenges in the Treatment of Acute Myeloid Leukemia. Genes & Cancer. 2011;2(2):95-107.
23. Steffen Bea. The molecular pathogenesis of acute myeloid leukemia. 2005;56:221.
24. Falini B, Martelli MP, Bolli N, et al. Acute myeloid leukemia with mutated nucleophosmin (NPM1): is it a distinct entity? Blood. 2011;117(4):1109-20.
25. Oki Y, Issa JP. Epigenetic mechanisms in AML - a target for therapy. Cancer Treat Res. 2010;145:19-40.
26. Lund AH, van Lohuizen M. Epigenetics and cancer. Genes Dev. 2004;18(19):2315-35.
27. Quintas-Cardama A, Santos FP, Garcia-Manero G. Histone deacetylase inhibitors for the treatment of myelodysplastic syndrome and acute myeloid leukemia. Leukemia. 2011;25(2):226-35.
28. Gottlicher M, Minucci S, Zhu P, et al. Valproic acid defines a novel class of HDAC inhibitors inducing differentiation of transformed cells. EMBO J. 2001;20(24):6969-78.
29. Delcuve GP, Khan DH, Davie JR. Roles of histone deacetylases in epigenetic regulation: emerging paradigms from studies with inhibitors. Clin Epigenetics. 2012;4(1):5.
30. Dokmanovic M, Clarke C, Marks PA. Histone deacetylase inhibitors: overview and perspectives. Mol Cancer Res. 2007;5(10):981-9.
31. Jung GA, Yoon JY, Moon BS, et al. Valproic acid induces differentiation and inhibition of proliferation in neural progenitor cells via the beta-catenin-Ras-ERK-p21Cip/WAF1 pathway. BMC Cell Biol. 2008;9:66.
32. Krämer OH, Zhu P, Ostendorff HP, et al. The histone deacetylase inhibitor valproic acid selectively induces proteasomal degradation of HDAC2. The EMBO Journal. 2003;22(13):3411-20.
33. Sefton BM. Overview of Protein Phosphorylation. . Current Protocols in Cell Biology. 1 May 2001 ed2001.
34. Schaab C, Oppermann FS, Klammer M, et al. Global phosphoproteome analysis of human bone marrow reveals predictive phosphorylation markers for the treatment of acute myeloid leukemia with quizartinib. Leukemia. 2014;28(3):716-9.
35. Maier T, Guell M, Serrano L. Correlation of mRNA and protein in complex biological samples. FEBS Lett. 2009;583(24):3966-73.
36. Berg JM, et.al. Biochemistry. 5th edition ed. New York: W. H. Freeman and Company; 2002.
37. Srivastava S, et.al. Molecular Pathology of Early Cancer. Netherlands: IOS Press; 1999. 481 p.
38. Milella M, Kornblau SM, Estrov Z, et al. Therapeutic targeting of the MEK/MAPK signal transduction module in acute myeloid leukemia. J Clin Invest. 2001;108(6):851-9.
39. Lunghi P, Tabilio A, Dall'Aglio PP, et al. Downmodulation of ERK activity inhibits the proliferation and induces the apoptosis of primary acute myelogenous leukemia blasts. Leukemia. 2003;17(9):1783-93.
40. Lowenberg B, Downing JR, Burnett A. Acute Myeloid Leukemia. New England Journal of Medicine. 1999;341(14):1051-62.
41. Burnett A, Wetzler M, Lowenberg B. Therapeutic advances in acute myeloid leukemia. J Clin Oncol. 2011;29(5):487-94.
42. de Greef GE, van Putten WL, Boogaerts M, et al. Criteria for defining a complete remission in acute myeloid leukaemia revisited. An analysis of patients treated in HOVON-SAKK co-operative group studies. Br J Haematol. 2005;128(2):184-91.
43. Rahman AM, Yusuf SW, Ewer MS. Anthracycline-induced cardiotoxicity and the cardiac-sparing effect of liposomal formulation. Int J Nanomedicine. 2007;2(4):567-83.
44. Hollingshead LM, Faulds D. Idarubicin. A review of its pharmacodynamic and pharmacokinetic properties, and therapeutic potential in the chemotherapy of cancer. Drugs. 1991;42(4):690-719.

45. Quintas-Cardama A, Ravandi F, Liu-Dumlao T, et al. Epigenetic therapy is associated with similar survival compared with intensive chemotherapy in older patients with newly diagnosed acute myeloid leukemia. Blood. 2012;120(24):4840-5.
46. Cahn JY, Labopin M, Mandelli F, et al. Autologous bone marrow transplantation for first remission acute myeloblastic leukemia in patients older than 50 years: a retrospective analysis of the European Bone Marrow Transplant Group. Blood. 1995;85(2):575-9.
47. Koreth J, Schlenk R, Kopecky KJ, et al. Allogeneic stem cell transplantation for acute myeloid leukemia in first complete remission: systematic review and meta-analysis of prospective clinical trials. JAMA. 2009;301(22):2349-61.
48. Forman SJ, Rowe JM. The myth of the second remission of acute leukemia in the adult. Blood. 2013;121(7):1077-82.
49. Blaise D, Vey N, Faucher C, et al. Current status of reduced-intensity-conditioning allogeneic stem cell transplantation for acute myeloid leukemia. Haematologica. 2007;92(4):533-41.
50. Shimoni A, Nagler A. Optimizing the conditioning regimen for allogeneic stem-cell transplantation in acute myeloid leukemia; dose intensity is still in need. Best Pract Res Clin Haematol. 2011;24(3):369-79.
51. Hiddemann W, Kern W, Schoch C, et al. Management of acute myeloid leukemia in elderly patients. J Clin Oncol. 1999;17(11):3569-76.
52. Pilatrino C, Cilloni D, Messa E, et al. Increase in platelet count in older, poor-risk patients with acute myeloid leukemia or myelodysplastic syndrome treated with valproic acid and all-trans retinoic acid. Cancer. 2005;104(1):101-9.
53. Blum W, Klisovic RB, Hackanson B, et al. Phase I study of decitabine alone or in combination with valproic acid in acute myeloid leukemia. J Clin Oncol. 2007;25(25):3884-91.
54. Raffoux E, Cras A, Recher C, et al. Phase 2 clinical trial of 5-azacitidine, valproic acid, and all-trans retinoic acid in patients with high-risk acute myeloid leukemia or myelodysplastic syndrome. Oncotarget. 2010;1(1):34-42.
55. Trus MR, Yang L, Suarez Saiz F, et al. The histone deacetylase inhibitor valproic acid alters sensitivity towards all trans retinoic acid in acute myeloblastic leukemia cells. Leukemia. 2005;19(7):1161-8.
56. Fredly H, Stapnes Bjornsen C, Gjertsen BT, et al. Combination of the histone deacetylase inhibitor valproic acid with oral hydroxyurea or 6-mercaptopurin can be safe and effective in patients with advanced acute myeloid leukaemia--a report of five cases. Hematology. 2010;15(5):338-43.
57. Wang ES. Treating acute myeloid leukemia in older adults. Hematology AM Soc Hematol Educ Program. 2014;2014(1):14-20.
58. Schmiegelow K, Bretton-Meyer U. 6-mercaptopurine dosage and pharmacokinetics influence the degree of bone marrow toxicity following high-dose methotrexate in children with acute lymphoblastic leukemia. Leukemia. 2001;15(1):74-9.
59. Peterson GM, Naunton M. Valproate: a simple chemical with so much to offer. J Clin Pharm Ther. 2005;30(5):417-21.
60. Phiel CJ, Zhang F, Huang EY, et al. Histone deacetylase is a direct target of valproic acid, a potent anticonvulsant, mood stabilizer, and teratogen. J Biol Chem. 2001;276(39):36734-41.
61. Martin M, Kettmann R, Dequiedt F. Class IIa histone deacetylases: regulating the regulators. Oncogene. 0000;26(37):5450-67.
62. Cheng YC, Lin H, Huang MJ, et al. Downregulation of c-Myc is critical for valproic acid-induced growth arrest and myeloid differentiation of acute myeloid leukemia. Leuk Res. 2007;31(10):1403-11.
63. Martens AC, Van Bekkum DW, Hagenbeek A. The BN acute myelocytic leukemia (BNML) (a rat model for studying human acute myelocytic leukemia (AML)). Leukemia. 1990;4(4):241-57.
64. McCormack E, Skavland J, Mujic M, et al. Lentinan: hematopoietic, immunological, and efficacy studies in a syngeneic model of acute myeloid leukemia. Nutr Cancer. 2010;62(5):574-83.
65. Hagenbeek A, Martens ACM. The proliferative state of normal hemopoietic stem cells during progression of leukemia. Studies in the BN acute myelocytic leukemia (BNML). Leukemia Research. 1981;5(2):141-8.

66. Wu W, Zhao S. Metabolic changes in cancer: beyond the Warburg effect. Acta Biochim Biophys Sin (Shanghai). 2013;45(1):18-26.
67. Vander Heiden MG, Cantley LC, Thompson CB. Understanding the Warburg effect: the metabolic requirements of cell proliferation. Science. 2009;324(5930):1029-33.
68. Miwa H, Shikami M, Goto M, et al. Leukemia cells demonstrate a different metabolic perturbation provoked by 2-deoxyglucose. Oncol Rep. 2013;29(5):2053-7.
69. Jang M, Kim SS, Lee J. Cancer cell metabolism: implications for therapeutic targets. Exp Mol Med. 2013;45:e45.
70. Mathupala SP, Ko YH, Pedersen PL. Hexokinase II: cancer's double-edged sword acting as both facilitator and gatekeeper of malignancy when bound to mitochondria. Oncogene. 2006;25(34):4777-86.
71. Raivio KO, Andersson LC. Glutamine requirements for purine metabolism in leukemic lymphoblasts. Leuk Res. 1982;6(1):111-5.
72. Palma F, Agostini D, Mason P, et al. Purification and characterization of the carboxyl-domain of human hexokinase type III expressed as fusion protein. Mol Cell Biochem. 1996;155(1):23-9.
73. Dang CV, Hamaker M, Sun P, et al. Therapeutic targeting of cancer cell metabolism. J Mol Med (Berl). 2011;89(3):205-12.
74. Tsai HJ, Wilson JE. Functional organization of mammalian hexokinases: both N- and C-terminal halves of the rat type II isozyme possess catalytic sites. Arch Biochem Biophys. 1996;329(1):17-23.
75. White TK, Wilson JE. Isolation and characterization of the discrete N- and C-terminal halves of rat brain hexokinase: retention of full catalytic activity in the isolated C-terminal half. Arch Biochem Biophys. 1989;274(2):375-93.
76. Wilson JE. Isozymes of mammalian hexokinase: structure, subcellular localization and metabolic function. J Exp Biol. 2003;206(Pt 12):2049-57.
77. John S, Weiss JN, Ribalet B. Subcellular localization of hexokinases I and II directs the metabolic fate of glucose. PLOS One. 2011;6(3):e17674.
78. Schindler A, Foley E. Hexokinase 1 blocks apoptotic signals at the mitochondria. Cell Signal. 2013;25(12):2685-92.
79. Chen Z, Zhang H, Lu W, et al. Role of mitochondria-associated hexokinase II in cancer cell death induced by 3-Bromopyruvate. Biochimica et Biophysica Acta. 2009;1787(5):553-60.
80. Hulleman E, Broekhuis MJ, Pieters R, et al. Pyruvate kinase M2 and prednisolone resistance in acute lymphoblastic leukemia. Haematologica. 2009;94(9):1322-4.
81. Christofk HR, Vander Heiden MG, Harris MH, et al. The M2 splice isoform of pyruvate kinase is important for cancer metabolism and tumour growth. Nature. 2008;452(7184):230-3.
82. Tong X, Zhao F, Thompson CB. The molecular determinants of de novo nucleotide biosynthesis in cancer cells. Curr Opin Genet Dev. 2009;19(1):32-7.
83. Albert B, et.al. Molecular Biology of the Cell. 5 ed. Granum MAaS, editor. 270 Madison Avenue, New York NY 10016, USA, and 2 Park Square, Milton Park, Abingdon, OX14 4RN, UK.: Garland Science, Taylor and Francis Group, LLC an informa business; 2008. 1268 p.
84. Hedstrom L. IMP dehydrogenase: structure, mechanism, and inhibition. Chem Rev. 2009;109(7):2903-28.
85. Lane AN, Fan TW. Regulation of mammalian nucleotide metabolism and biosynthesis. Nucleic Acids Res. 2015;43(4):2466-85.
86. Galmarini CM, et-al. Nucleoside analogues: mechanisms of drug resistance and reversal strategies. 2001;15(6):890.
87. Nagai M, Natsumeda Y, Konno Y, et al. Selective up-regulation of type II inosine 5'-monophosphate dehydrogenase messenger RNA expression in human leukemias. Cancer Res. 1991;51(15):3886-90.
88. Jain J, Almquist SJ, Ford PJ, et al. Regulation of inosine monophosphate dehydrogenase type I and type II isoforms in human lymphocytes. Biochem Pharmacol. 2004;67(4):767-76.

89. Konno Y, Natsumeda Y, Nagai M, et al. Expression of human IMP dehydrogenase types I and II in Escherichia coli and distribution in human normal lymphocytes and leukemic cell lines. J Biol Chem. 1991;266(1):506-9.
90. Goldstein BM, Leary JF, Farley BA, et al. Induction of HL60 cell differentiation by tiazofurin and its analogues: characterization and efficacy. Blood. 1991;78(3):593-8.
91. Pospisilova J, Vit O, Lorkova L, et al. Resistance to TRAIL in mantle cell lymphoma cells is associated with the decreased expression of purine metabolism enzymes. Int J Mol Med. 2013;31(5):1273-9.
92. Bentley R. Mycophenolic Acid: a one hundred year odyssey from antibiotic to immunosuppressant. Chem Rev. 2000;100(10):3801-26.
93. Allison AC, Eugui EM. Mycophenolate mofetil and its mechanisms of action. Immunopharmacology. 2000;47(2-3):85-118.
94. Allison AC, Watts RWE, Hovi T, et al. IMMUNOLOGICAL OBSERVATIONS ON PATENTS WITH LESCH-NYHAN SYNDROME, AND ON THE ROLE OF DE-NOVO PURINE SYNTHESIS IN LYMPHOCYTE TRANSFORMATION. The Lancet. 1975;306(7946):1179-83.
95. Allison AC, Kowalski, W.J., Muller, C. D., Eugui, E. M. . Mechanisms of Action of Mycophenolic Acid. 1993;696:87.
96. Gu JJ, Santiago L, Mitchell BS. Synergy between imatinib and mycophenolic acid in inducing apoptosis in cell lines expressing Bcr-Abl2005 2005-04-15 00:00:00. 3270-7 p.
97. Collart FR, Huberman E. Expression of IMP dehydrogenase in differentiating HL-60 cells. Blood. 1990;75(3):570-6.
98. Nista A, De Martino C, Malorni W, et al. Effect of lonidamine on the aerobic glycolysis of normal and phytohemagglutinin-stimulated human peripheral blood lymphocytes. Exp Mol Pathol. 1985;42(2):194-205.
99. Floridi A, Lehninger AL. Action of the antitumor and antispermatogenic agent lonidamine on electron transport in Ehrlich ascites tumor mitochondria. Arch Biochem Biophys. 1983;226(1):73-83.
100. Floridi A, Paggi MG, D'Atri S, et al. Effect of lonidamine on the energy metabolism of Ehrlich ascites tumor cells. Cancer Res. 1981;41(11 Pt 1):4661-6.
101. Gottlob K, Majewski N, Kennedy S, et al. Inhibition of early apoptotic events by Akt/PKB is dependent on the first committed step of glycolysis and mitochondrial hexokinase. Genes & Development. 2001;15(11):1406-18.
102. Watabe M, Masuda Y, Nakajo S, et al. The cooperative interaction of two different signaling pathways in response to bufalin induces apoptosis in human leukemia U937 cells. J Biol Chem. 1996;271(24):14067-72.
103. Calvino E, Estan MC, Simon GP, et al. Increased apoptotic efficacy of lonidamine plus arsenic trioxide combination in human leukemia cells. Reactive oxygen species generation and defensive protein kinase (MEK/ERK, Akt/mTOR) modulation. Biochem Pharmacol. 2011;82(11):1619-29.
104. Jin G, Bausch D, Thomas K, et al. Histone deacetylase inhibitors enhance endothelial cell sprouting angiogenesis in vitro. Surgery. 2011;150(3):429-35.
105. Ning SC, Hahn GM. Cytotoxicity of lonidamine alone and in combination with other drugs against murine RIF-1 and human HT1080 cells in vitro. Cancer Res. 1990;50(24):7867-70.
106. Del Bufalo D, Biroccio A, Soddu S, et al. Lonidamine induces apoptosis in drug-resistant cells independently of the p53 gene. J Clin Invest. 1996;98(5):1165-73.
107. De Lena M, Lorusso V, Bottalico C, et al. Revertant and potentiating activity of lonidamine in patients with ovarian cancer previously treated with platinum. J Clin Oncol. 1997;15(10):3208-13.
108. Oudard S, Carpentier A, Banu E, et al. Phase II study of lonidamine and diazepam in the treatment of recurrent glioblastoma multiforme. J Neurooncol. 2003;63(1):81-6.
109. Mansi JL, de Graeff A, Newell DR, et al. A phase II clinical and pharmacokinetic study of Lonidamine in patients with advanced breast cancer. Br J Cancer. 1991;64(3):593-7.
110. Sanchez Y, Simon GP, Calvino E, et al. Curcumin stimulates reactive oxygen species production and potentiates apoptosis induction by the antitumor drugs arsenic trioxide and lonidamine in human myeloid leukemia cell lines. J Pharmacol Exp Ther. 2010;335(1):114-23.

111. Estan MC, Calvino E, Calvo S, et al. Apoptotic efficacy of etomoxir in human acute myeloid leukemia cells. Cooperation with arsenic trioxide and glycolytic inhibitors, and regulation by oxidative stress and protein kinase activities. PLOS One. 2014;9(12):e115250.
112. Scorza Barcellona P, Campana A, Silvestrini B, et al. The embryotoxicity of a new class of antispermatogenic agents: the 3-indazole-carboxylic acids. Arch Toxicol Suppl. 1982;5:197-201.
113. Bruserud O, Gjertsen BT, Foss B, et al. New strategies in the treatment of acute myelogenous leukemia (AML): in vitro culture of aml cells--the present use in experimental studies and the possible importance for future therapeutic approaches. Stem Cells. 2001;19(1):1-11.
114. Leibniz-Institut DSMZ-Deutsche Sammlung von Mikroorganismen und Zellkulturen GmbH [Catalogue]. Available from: http://www.dsmz.de/catalogues/details/culture/ACC-554.html.
115. Wolf D, Rotter V. Major deletions in the gene encoding the p53 tumor antigen cause lack of p53 expression in HL-60 cells. Proc Natl Acad Sci U S A. 1985;82(3):790-4.
116. Lanotte M, Martin-Thouvenin V, Najman S, et al. NB4, a maturation inducible cell line with t(15;17) marker isolated from a human acute promyelocytic leukemia (M3). Blood. 1991;77(5):1080-6.
117. Simione FP. Thermo Scientific Nalgene and Nunc Cryopreservation Guide. www.thermoscientific.com/coldstorage2009. p. 16.
118. Agliano A, et.al. Huma acute leukemia cells injected in NOD/LtSz-scid/IL-2Rγ null mice generate a faster an more efficient disease compared to other NOD/scid-related strains. 2008;123:2227.
119. General information on laws and regulations University of Bergen Homepage: The Laboratory Animal Facility. Available from: http://www.uib.no/en/rg/animalfacility/67407/general-information-laws-and-regulations.
120. McVicar N, Li AX, Meakin SO, et al. Imaging chemical exchange saturation transfer (CEST) effects following tumor-selective acidification using lonidamine. NMR Biomed. 2015;28(5):566-75.
121. Kahler CP. Evaluation of the use of the solvent dimethyl sulfoxide in chemiluminescent studies. Blood Cells Mol Dis. 2000;26(6):626-33.
122. Berridge MV, Tan AS. Trans-plasma membrane electron transport: A cellular assay for NADH- and NADPH-oxidase based on extracellular, superoxide-mediated reduction of the sulfonated tetrazolium salt WST-1. Protoplasma. 1998;205(1-4):74-82.
123. Kepp O, Galluzzi L, Lipinski M, et al. Cell death assays for drug discovery. Nat Rev Drug Discov. 2011;10(3):221-37.
124. Fadok VA, Bratton DL, Frasch SC, et al. The role of phosphatidylserine in recognition of apoptotic cells by phagocytes. Cell Death Differ. 1998;5(7):551-62.
125. Dubois T, Mira JP, Feliers D, et al. Annexin V inhibits protein kinase C activity via a mechanism of phospholipid sequestration. Biochemical Journal. 1998;330(Pt 3):1277-82.
126. PhosphoProtein Handbook. In: Qiagen®, editor. Second Edition ed. www.qiagen.comJuly 2011. p. 22.
127. Bradford MM. A rapid and sensitive method for the quantitation of microgram quantities of protein utilizing the principle of protein-dye binding. Anal Biochem. 1976;72:248-54.
128. Bagrintseva K, Geisenhof S, Kern R, et al. FLT3-ITD-TKD dual mutants associated with AML confer resistance to FLT3 PTK inhibitors and cytotoxic agents by overexpression of Bcl-x(L). Blood. 2005;105(9):3679-85.
129. Figg WD, Walls RG, Cooper MR, et al. In vitro antitumor effect of hydroxyurea on hormone-refractory prostate cancer cells and its potentiation by phenylbutyrate. Anticancer Drugs. 1994;5(3):336-42.
130. Teicher BA. Lonidamine: in vitro/in vivo correlations. Eur J Cancer. 1994;30A(10):1411-3.
131. Shoucheng Ning GMH. Cytotoxicity of Lonidamine alone and in combination with other drugs against murine RIF-1 and human HT1080 cells in vitro. 1990;50:7870.
132. Rika Kawagoe HK, Kimihiko Sano. Valproic acid induces apoptosis in human leukemia cells by stimulating both caspase-dependent and -independent apoptotic signaling pathways. 2002;26:502.

133. Riva G, Baronchelli S, Paoletta L, et al. In vitro anticancer drug test: A new method emerges from the model of glioma stem cells. Toxicology Reports. 2014;1(0):188-99.
134. M R Trus LY, F Suarez Saiz, L Bordeleau, I Jurisica, M D Minden. The histone deacetylase inhibitor valproic acid alters sensitivity towards all trans retinioic acid in acute myeloblastic leukemia cells. 2005;19:1168.
135. Millon SR, Ostrander JH, Brown JQ, et al. Uptake of 2-NBDG as a method to monitor therapy response in breast cancer cell lines. Breast Cancer Res Treat. 2011;126(1):55-62.
136. Gitenay D, Wiel C, Lallet-Daher H, et al. Glucose metabolism and hexosamine pathway regulate oncogene-induced senescence. Cell Death Dis. 2014;5:e1089.
137. Weber G. Biochemical strategy of cancer cells and the design of chemotherapy: G. H. A. Clowes Memorial Lecture. Cancer Res. 1983;43(8):3466-92.
138. Zeevi A, Woan M, Yao GZ, et al. Comparative In Vitro Studies on the Immunosuppressive Activities of Mycophenolic Acid, Bredinin, FK 506, Cyclosporine, and Rapamycin. Transplantation proceedings. 1991;23(6):2928-30.
139. Eugui EM, Almquist SJ, Muller CD, et al. Lymphocyte-selective cytostatic and immunosuppressive effects of mycophenolic acid in vitro: role of deoxyguanosine nucleotide depletion. Scand J Immunol. 1991;33(2):161-73.
140. Messina E, Gazzaniga P, Micheli V, et al. Low levels of mycophenolic acid induce differentiation of human neuroblastoma cell lines. International Journal of Cancer. 2004;112(2):352-4.
141. Bratton DL, Fadok VA, Richter DA, et al. Polyamine regulation of plasma membrane phospholipid flip-flop during apoptosis. J Biol Chem. 1999;274(40):28113-20.
142. Kleffel S, Schatton T. Tumor dormancy and cancer stem cells: two sides of the same coin? Adv Exp Med Biol. 2013;734:145-79.
143. Torres RJ, Puig JG, Jinnah HA. Update on the Phenotypic Spectrum of Lesch-Nyhan Disease and its Attenuated Variants. Current rheumatology reports. 2012;14(2):189-94.
144. Annapandian VM, John GT, Mathew BS, et al. Pharmacokinetic interaction between sodium valproate and mycophenolate in renal allograft recipients. Transplantation. 2009;88(9):1143-5.
145. Debetto P, Bianchi V. Reversed-phase high-performance liquid chromatographic analysis of endogenous purine ribonucleotide pools in BHK monolayer cultures. Journal of High Resolution Chromatography. 1983;6(3):117-22.
146. López-Lázaro M. A New View of Carcinogenesis and an Alternative Approach to Cancer Therapy. Molecular Medicine. 2010;16(3-4):144-53.
147. Stapnes C, Ryningen A, Hatfield K, et al. Functional characteristics and gene expression profiles of primary acute myeloid leukaemia cells identify patient subgroups that differ in susceptibility to histone deacetylase inhibitors. Int J Oncol. 2007;31(6):1529-38.
148. Fredly H, Gjertsen BT, Bruserud O. Histone deacetylase inhibition in the treatment of acute myeloid leukemia: the effects of valproic acid on leukemic cells, and the clinical and experimental evidence for combining valproic acid with other antileukemic agents. Clin Epigenetics. 2013;5(1):12.
149. Reuss-Borst MA, Bühring HJ, Klein G, et al. Adhesion molecules on CD 34+ hematopoietic cells in normal human bone marrow and leukemia. Annals of Hematology. 1992;65(4):169-74.
150. Renneville A, Roumier C, Biggio V, et al. Cooperating gene mutations in acute myeloid leukemia: a review of the literature. Leukemia. 2008;22(5):915-31.
151. Haas R, Stumpf DA, Parks JK, et al. Inhibitory effects of sodium valproate on oxidative phosphorylation. Neurology. 1981;31(11):1473-6.
152. Bryson JM, Coy PE, Gottlob K, et al. Increased hexokinase activity, of either ectopic or endogenous origin, protects renal epithelial cells against acute oxidant-induced cell death. J Biol Chem. 2002;277(13):11392-400.
153. Prezma T, Shteinfer A, Admoni L, et al. VDAC1-based peptides: novel pro-apoptotic agents and potential therapeutics for B-cell chronic lymphocytic leukemia. Cell Death Dis. 2013;4:e809.
154. Parrish AB, Freel CD, Kornbluth S. Cellular mechanisms controlling caspase activation and function. Cold Spring Harb Perspect Biol. 2013;5(6).

155. Allan LA, Morrice N, Brady S, et al. Inhibition of caspase-9 through phosphorylation at Thr 125 by ERK MAPK. Nat Cell Biol. 2003;5(7):647-54.
156. Cardone MH, Roy N, Stennicke HR, et al. Regulation of cell death protease caspase-9 by phosphorylation. Science. 1998;282(5392):1318-21.
157. Wang C, Luan Z, Yang Y, et al. Valproic acid induces apoptosis in differentiating hippocampal neurons by the release of tumor necrosis factor-alpha from activated astrocytes. Neurosci Lett. 2011;497(2):122-7.
158. Noh JH, Jung KH, Kim JK, et al. Aberrant Regulation of HDAC2 Mediates Proliferation of Hepatocellular Carcinoma Cells by Deregulating Expression of G1/S Cell Cycle Proteins. PLOS One. 2011;6(11):e28103.
159. Oudard S, Poirson F, Miccoli L, et al. Mitochondria-bound hexokinase as target for therapy of malignant gliomas. Int J Cancer. 1995;62(2):216-22.
160. Nath K, Nelson DS, Heitjan DF, et al. Effects of hyperglycemia on lonidamine-induced acidification and de-energization of human melanoma xenografts and sensitization to melphalan. NMR Biomed. 2015;28(3):395-403.
161. Thackaberry EA, Wang X, Schweiger M, et al. Solvent-based formulations for intravenous mouse pharmacokinetic studies: tolerability and recommended solvent dose limits. Xenobiotica. 2014;44(3):235-41.
162. Nath K, Nelson DS, Ho AM, et al. (31) P and (1) H MRS of DB-1 melanoma xenografts: lonidamine selectively decreases tumor intracellular pH and energy status and sensitizes tumors to melphalan. NMR Biomed. 2013;26(1):98-105.
163. Konovalova NP. Ultralow Doses of Various Drugs in Chemotherapy of Experimental Tumors. Bulletin of Experimental Biology and Medicine. 2003;135(7):45-7.
164. Fanciulli M, Bruno T, Giovannelli A, et al. Energy metabolism of human LoVo colon carcinoma cells: correlation to drug resistance and influence of lonidamine. Clin Cancer Res. 2000;6(4):1590-7.
165. Petrucci MT, Levi A, Bringhen S, et al. Bortezomib, melphalan, and prednisone in elderly patients with relapsed/refractory multiple myeloma: a multicenter, open label phase 1/2 study. Cancer. 2013;119(5):971-7.